Interfacing analytical and numerical relativity in modeling binary black-hole coalescences

Alessandra Buonanno

Department of Physics, University of Maryland

Caltech - JPL Association for Gravitational Wave Research (CaJAGWR)

Motivation/outline

Interfacing analytical and numerical relativity computations to *grasp* the two-body problem, *model* the dynamics and the gravitational-wave emission, with the goal of

- **understanding gravity in the weak and strong regime**

  e.g., comparing with post-Newtonian theory; interpret the transition inspiral to merger to ringdown; non linearities

- **detecting gravitational waves and extract unique information**

  e.g., building effective and faithful templates

- **making astrophysical predictions**

  e.g., recoil velocity of merging black holes; how supermassive black holes formed

Two-body problem in general relativity

Solving the Einstein field equations $R_{\mu\nu} - \frac{1}{2}\, g_{\mu\nu}\, R = \frac{8\pi G}{c^4}\, T_{\mu\nu}$

Computing the radiation field h_{ij}^{TT}

- **analytically, through approximation schemes**
  - **test-particle limit ($m_2/m_1 \ll 1$)**
  - **slow motion ($1/c$)**
  - **weak field (G)**

- **numerically, with a computer**
  - **spacetime metric** $ds^2 = g_{\mu\nu}\, dx^\mu\, dx^\nu$
  - **10 coupled non-linear differential equations depending on 4 spacetime coordinates**

Test-particle falling radially in a Schwarzschild black hole

$$\frac{d^2}{dr_*^2} Z_l + (V_l - \omega^2)\, Z_l = \mathcal{S}_l$$

$Z_l \longrightarrow$ perturbation $\quad \mathcal{S}_l \longrightarrow$ source

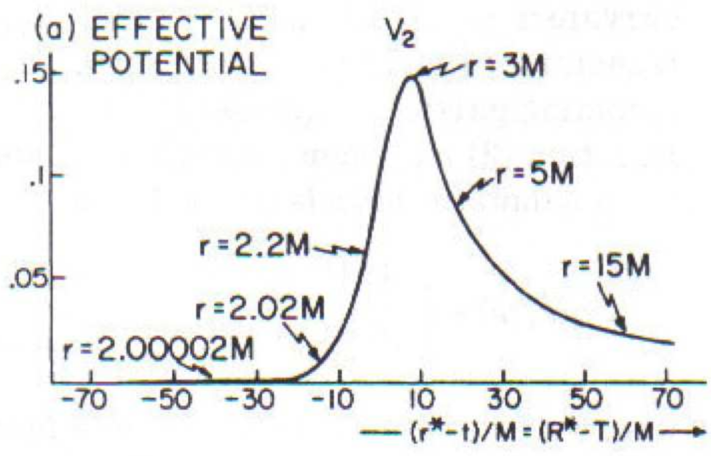

Outgoing field

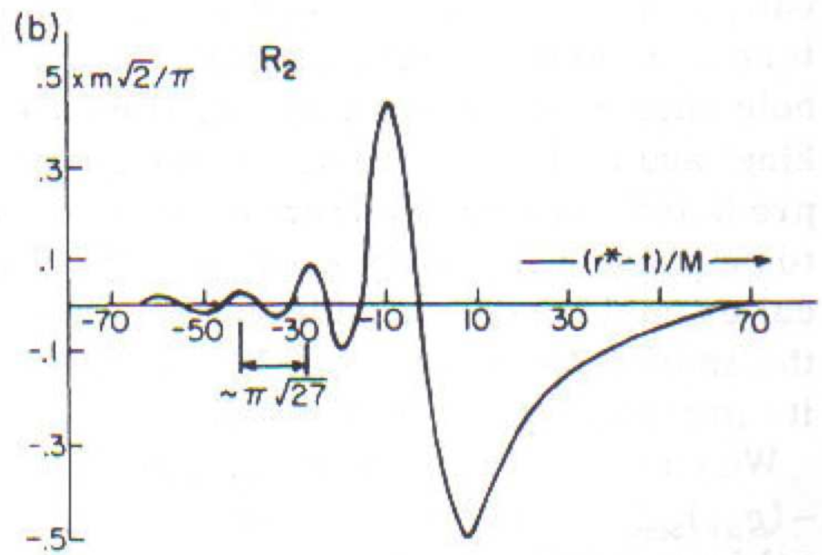

... part of the energy produced in the strong-burst region is stored in the resonant cavity of the geometry, and then slowly released in ringdown modes.

[Press 71; Davis, Ruffini, Press & Price 71; Davis, Ruffini & Tionmo 72]

Black-hole perturbations and quasi-normal modes

- **Perturbations of Schwarzschild:** $\frac{d^2}{dr_*^2} Z_l + (V_l - \omega^2)\, Z_l = \mathcal{S}_l$

  [Regge & Wheeler 57; Zerilli 70; Bardeen & Press 73]

- **Black-hole quasi-normal modes:** $\mathcal{S} = 0$, **no incoming radiation** $\mathcal{A}\, e^{-i\omega\, r_*} \quad r_* \to +\infty$

  $\mathcal{B}\, e^{+i\omega\, r_*} \quad r_* \to -\infty$

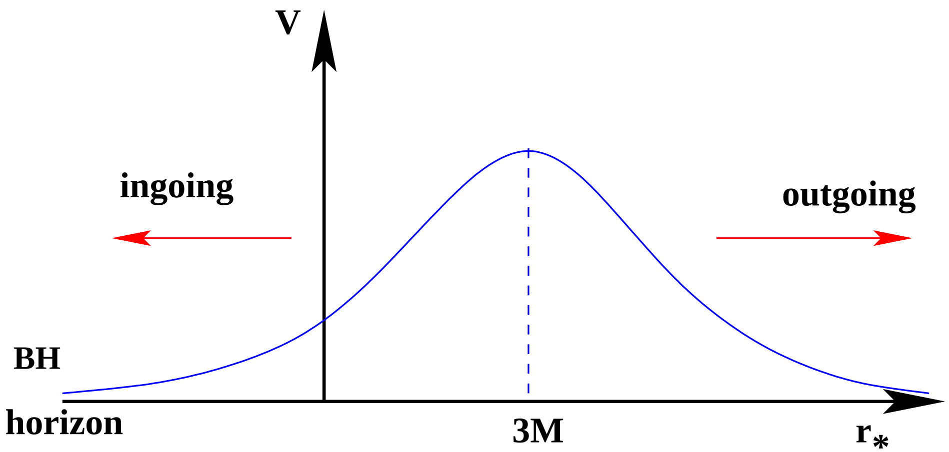

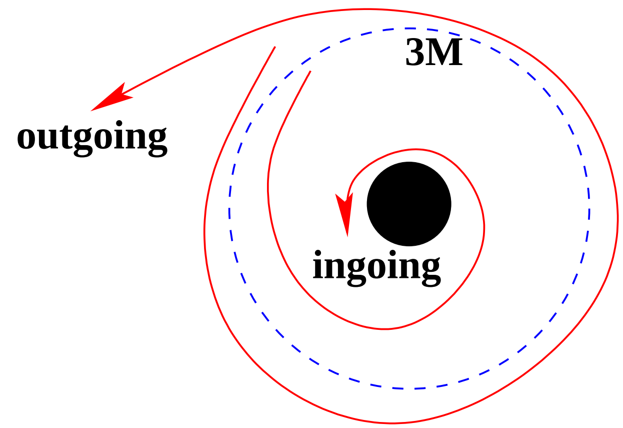

Peak of the curvature potential close to the Schwarzschild light-ring $r = 3M$

$\mathrm{Re}[\omega_{lm0}^{\rm QNM}] \sim \sqrt{V_l^{\rm peak}} \sim \frac{l}{\sqrt{27}M}$ **and if** $l = 2$ $\mathrm{Re}[\omega_{220}^{\rm QNM}] \sim 2\omega_{\rm LR}$

[Vishveshwara 70; Press 71; Chandrasekhar & Detweiler 75; Schutz & Will 85]

Close-limit approximation for head-on collision and Lazarus project

- **Close-limit approximation** [Price & Pullin 94]

  Switch from a two-body to a one-body description and use BH perturbation theory to describe the subsequent evolution

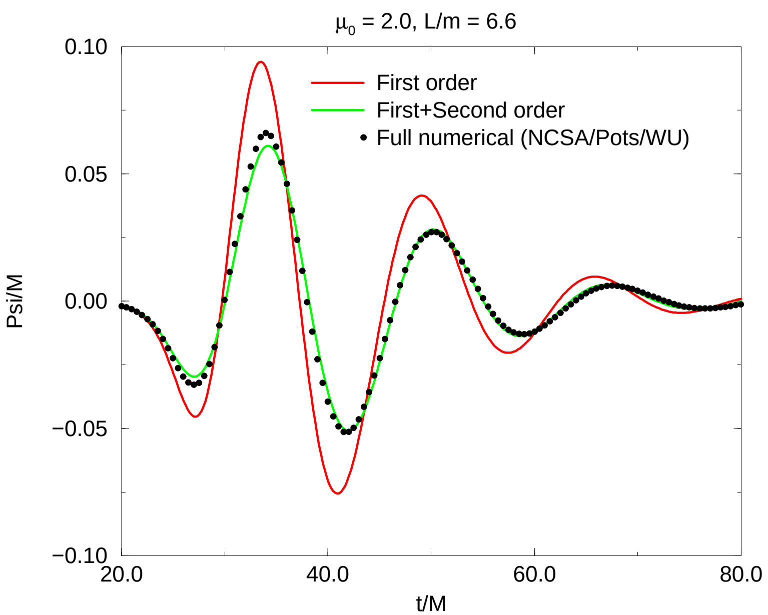

[Anninos et al. 95]

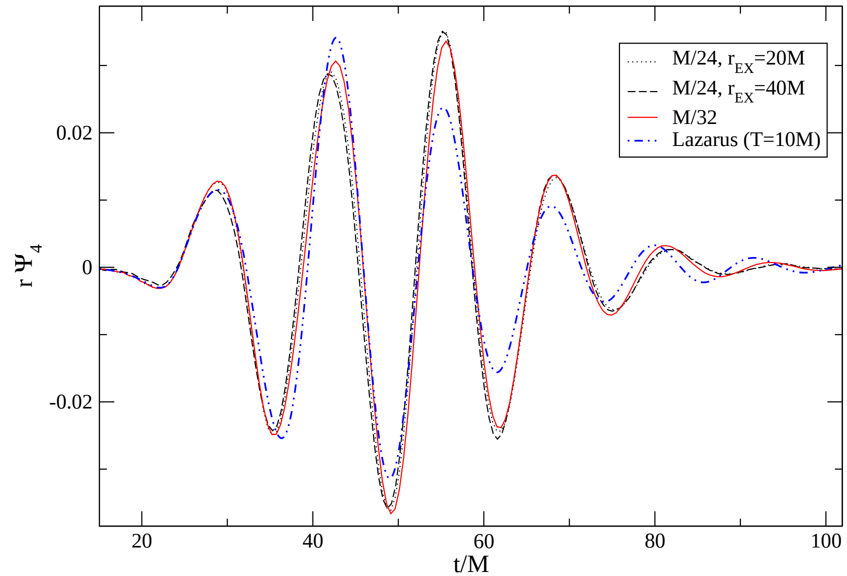

- **Lazarus project**

[Baker, Brügmann, Campanelli & Lousto 01]

Modeling the long inspiral phase using PN theory

- **In general relativity radiation-reaction effects appear at order $\sim v^5/c^5$ beyond the Newtonian force law**

$$m\,\frac{d\mathbf{v}}{dt} = \mathbf{F}_{\rm Newt} + \cdots + \left(\frac{v}{c}\right)^5 \mathbf{F}_{\rm RR}$$

- **Throughout the inspiral $T_{\rm RR} \gg T_{\rm orb} \Rightarrow$ natural** *adiabatic parameter*

$$\frac{\dot{\omega}}{\omega^2} = \mathcal{O}\left[\left(\frac{v}{c}\right)^5\right]$$

- **PN expansion: formal expansion in $1/c$ when $c \to +\infty$**

- **For compact bodies, such as neutron stars and black holes,**

$$\frac{v^2}{c^2} \sim \frac{Gm}{c^2 r} \sim \frac{R_S}{r} \ll 1$$

Waveforms in the adiabatic approximation

- **Inspiral as an adiabatic sequence of circular orbits:**

$$h(t) \propto \ddot{Q} \propto \frac{v^2}{c^2} \cos 2\varphi \propto \left(\frac{Gm\,\omega}{c^3}\right)^{2/3} \cos 2\varphi$$

- **Energy-balance equation:** $\frac{dE(v)}{dt} = -F(v)$

$E(v) \rightarrow$ center-of-mass energy $\quad F(v) \rightarrow$ gravitational-wave energy flux

$E(v)$ **and** $F(v)$ **known as a PN expansion in** $v/c = (Gm\omega/c^3)^{1/3}$

$$\Rightarrow \dot{\omega} = -\frac{F(\omega)}{[dE(\omega)/d\omega]} \quad \Rightarrow \quad \varphi_{\rm GW}(t) = 2\varphi(t) = 1/\pi \int \omega\, dt$$

Effective-one-body approach [AB & Damour 99]

- **Resum the PN expansion assuming that the equal-mass limit is a η-deformation of the test-mass limit**
- **Resum in a coordinate invariant manner**
- **Resum so that known test mass limit results are recovered**

$\mu = m_1 \, m_2 / M$

$\eta = m_1 \, m_2 / M^2$

$0 \leq \eta \leq 1/4$

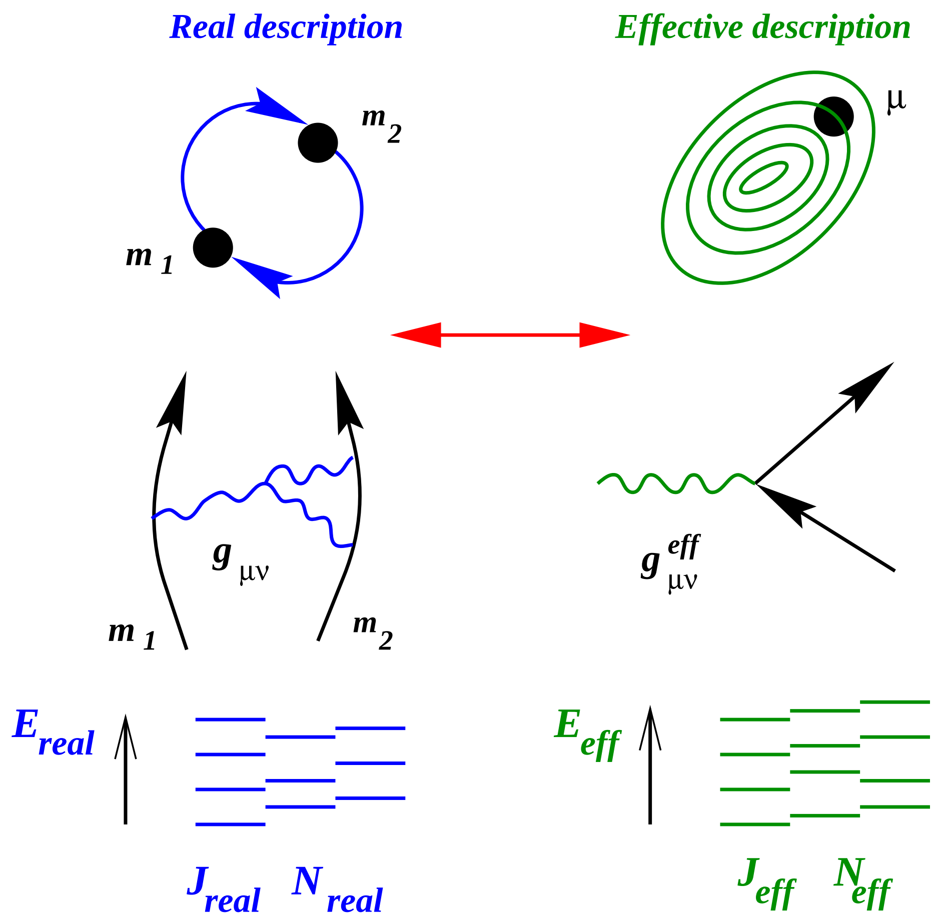

Rules to map real to effective problem

Quite natural to impose:

$$m_0 = \mu \qquad M_0 = M$$

$$J_{\rm eff} = J_{\rm real} \quad \& \quad \mathcal{N}_{\rm eff} = \mathcal{N}_{\rm real} \quad \text{with } \mathcal{N} = I + J$$

Allow transformation energy axis: $E_{\rm eff} = f(E_{\rm real})$

$$\frac{E_{\rm eff}^{\rm NR}}{m_0\, c^2} = \frac{E_{\rm real}^{\rm NR}}{\mu\, c^2}\left[1 + \alpha_1 \frac{E_{\rm real}^{\rm NR}}{\mu\, c^2} + \alpha_2 \left(\frac{E_{\rm real}^{\rm NR}}{\mu\, c^2}\right)^2 + \cdots\right]$$

Result from matching the energy

$$\frac{E_{\rm eff}^{\rm NR}}{m_0\,c^2} = \frac{E_{\rm real}^{\rm NR}}{\mu\,c^2}\left(1+\frac{\eta}{2}\,\frac{E_{\rm real}^{\rm NR}}{\mu\,c^2}\right)$$

Classical gravity (up to 3PN order)

$$E_{\rm real}^2 = m_1^2 + m_2^2 + 2m_1\,m_2\left(\frac{E_{\rm eff}}{\mu}\right)$$

Quantum electrodynamics (eikonal approximation) [Brézin, Itzykson & Zinn-Justin 70]

$$E_{\rm real}^2 = m_1^2 + m_2^2 + 2m_1\,m_2\,\frac{1}{\sqrt{1+Z^2\alpha^2/(n-\epsilon_j)^2}}$$

EOB approach: resummed Hamiltonian (non-spinning black holes)

[AB & Damour 99; Damour, Jaranowski & Schaefer 00]

"Effective" description

"Real" description

$$\mathcal{H}_{\rm real}(\boldsymbol{Q},\boldsymbol{P}) \sim M\left\{1+\eta\left[\frac{\boldsymbol{P}^2}{2}+\frac{M}{Q}\right]+c_4\,\boldsymbol{P}^4+\cdots\right\}$$

$$\mathcal{H}_{\rm eff}^{\eta}(\boldsymbol{q},\boldsymbol{p}) = \sqrt{A_\eta(q)\,\left[1+\boldsymbol{p}^2+\left(\frac{A_\eta(q)}{D_\eta(q)}-1\right)\,(\boldsymbol{n}\cdot\boldsymbol{p})^2+\mathcal{T}_4(\boldsymbol{p})\right]}$$

$$\boxed{\mathcal{H}_{\rm real}^{\rm impr}(\boldsymbol{Q},\boldsymbol{P}) = \sqrt{1+2\eta\,\left(\mathcal{H}_{\rm eff}^{\eta}(\boldsymbol{q},\boldsymbol{p})-1\right)}}$$

$$ds_{\rm eff}^2 = -A_\eta(q)\,dt^2+\frac{D_\eta(q)}{A_\eta(r)}\,dq^2+q^2\,d\Omega^2$$

- **Canonical transformation:** $\boldsymbol{q}=\mathcal{Q}(\boldsymbol{Q},\boldsymbol{P})$, $\boldsymbol{p}=\mathcal{P}(\boldsymbol{Q},\boldsymbol{P})$
- **All dynamics condensed in $A_\eta(q)$ and $D_\eta(q)$! Apply Padé resummation.**

New resummed *orbital energy* function: $E_{\rm real}^{\rm impr}(v)$

Comparing EOB- and PN-approximants to the binding energy

[AB 02]

equal-mass case

EOB-approximants

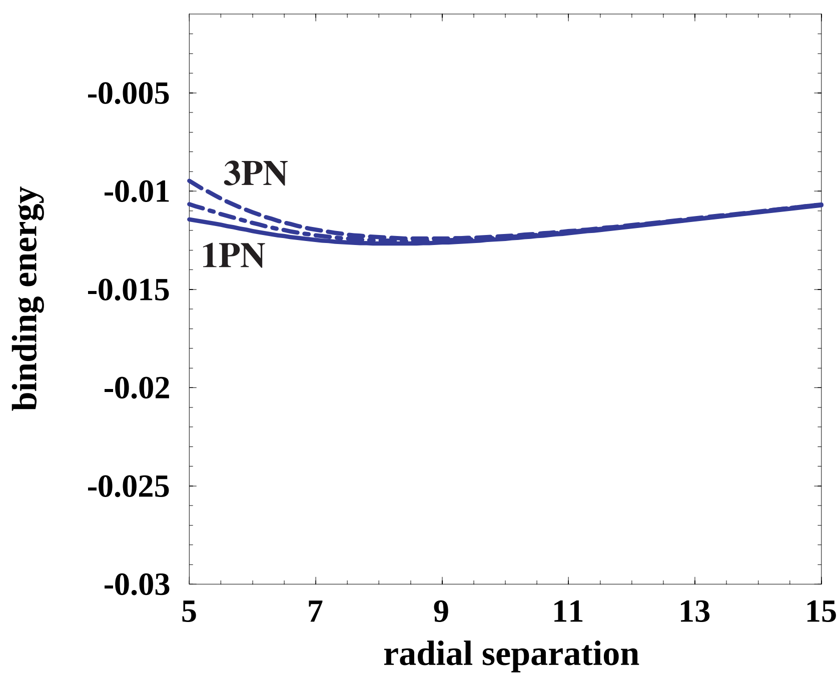

PN-approximants

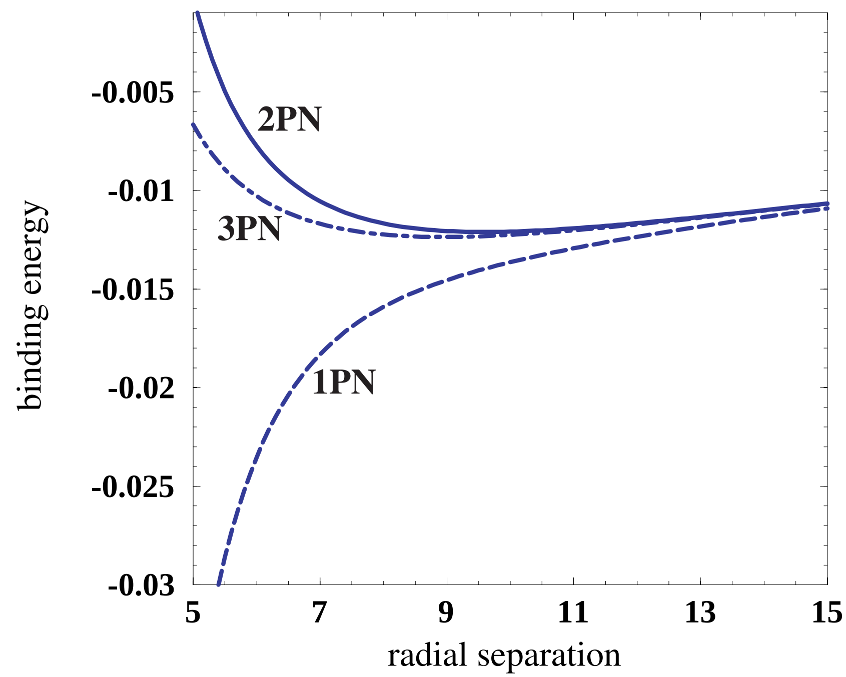

EOB approach: incorporating radiation reaction effects

[AB & Damour 00; AB, Chen & Damour 05]

$$\frac{dq^i}{dt} = \frac{\partial \mathcal{H}^{\rm impr}}{\partial p_i} \qquad \frac{dp_i}{dt} = -\frac{\partial \mathcal{H}^{\rm impr}}{\partial q^i} + \mathcal{F}_i$$

- **Assumptions: quasi-circular orbits and leading spin-dependent terms**
- **Radiation-reaction force matches known rates of energy and angular momentum loss for quasi-adiabatic orbits**
- **Padé resummation of the GW flux including spin effects**

[Damour, Sathyaprakash & Iyer 98; Porter & Sathyaprakash 04; AB, Chen & Damour 05]

What we learned from the EOB model

- **The plunge (~ 1.5 GW cycles) is a smooth continuation of the inspiral phase**
- **The transition merger to ringdown was assumed** *very short*
- One single **QNM matched using** $M_{\rm BH} = E_{\rm LR} = 0.976\, M$, $a_{\rm BH} = \boldsymbol{J}_{\rm LR}/E_{\rm LR}^2 = 0.77$

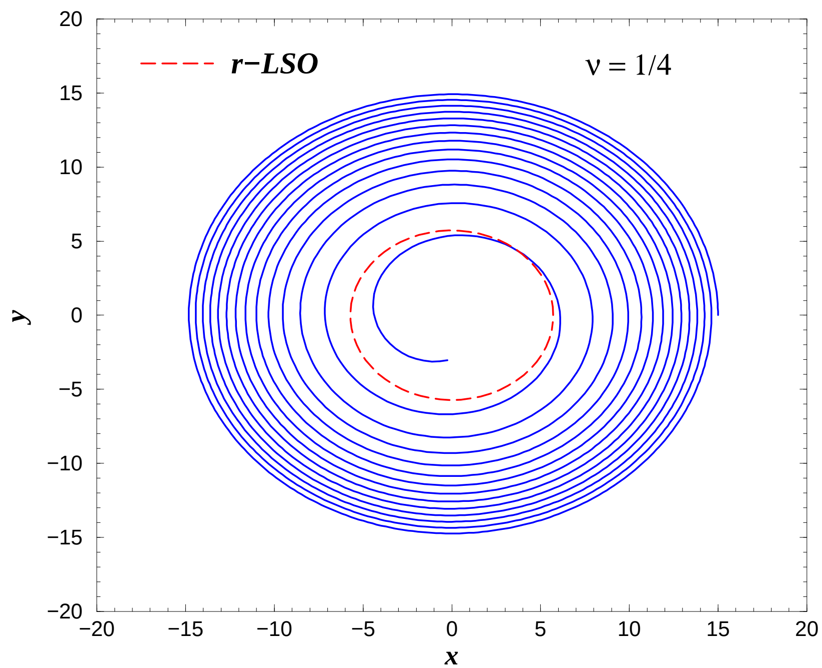

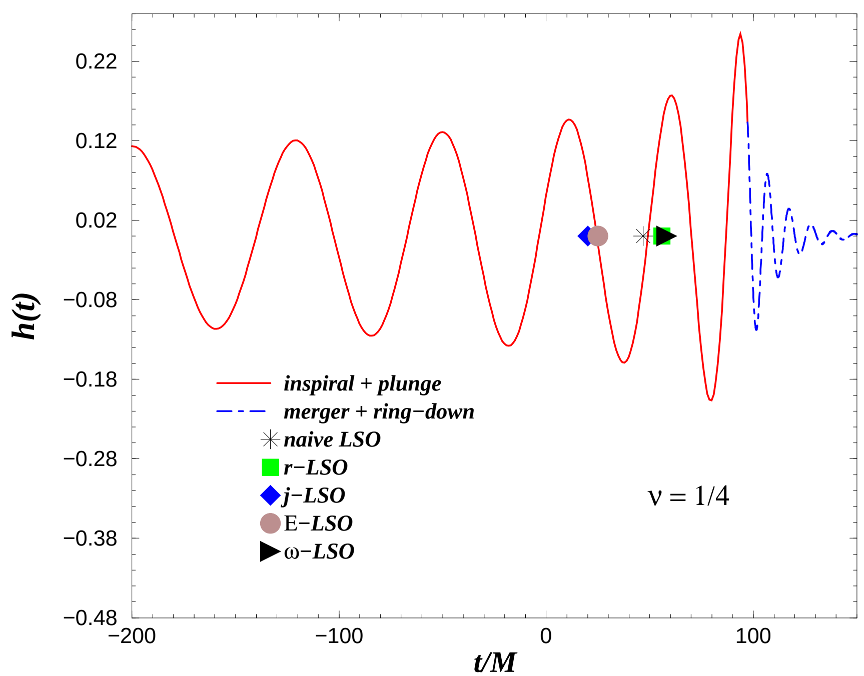

[AB & Damour 99, 00]

NR simulations for equal-mass binaries: quasi-circular evolution

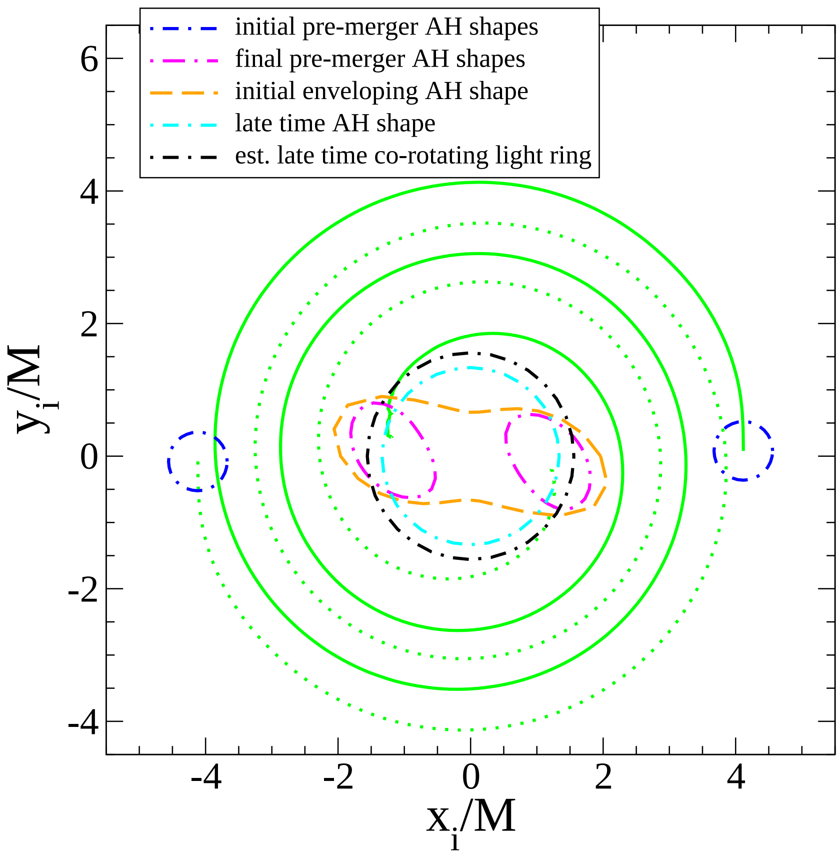

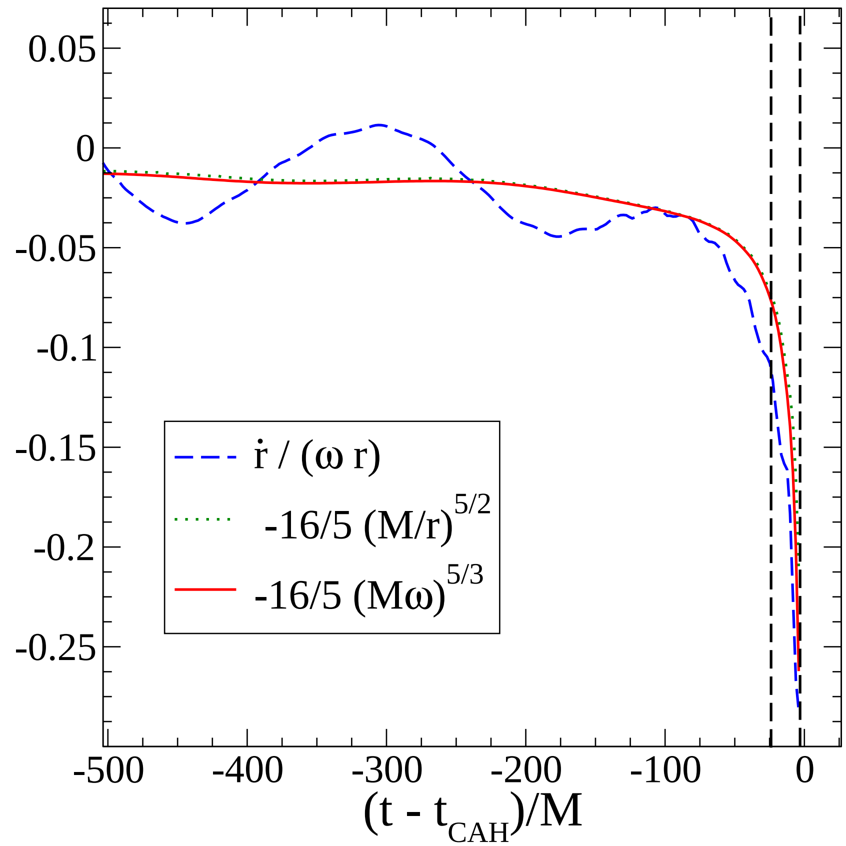

[AB, Cook & Pretorius 06]

ψ_4 and its multipole decomposition

$$\ddot{h}_+ = \frac{1}{2}(\ddot{h}^{TT}_{\hat{\theta}\hat{\theta}} - \ddot{h}^{TT}_{\hat{\phi}\hat{\phi}}) \qquad \ddot{h}_\times = \ddot{h}^{TT}_{\hat{\theta}\hat{\phi}} \qquad \Psi_4 = \ddot{h}_+ - i\ddot{h}_\times$$

Introducing the spin-weight -2 *spherical* **harmonics**: ${}_sY_{\ell m}(\theta,\phi)$

$$\Psi_4(t,\vec{r}) = \sum_{\ell m} {}_{-2}C_{\ell m}(t,r)\,{}_{-2}Y_{\ell m}(\theta,\phi)$$

Newtonian quasi-circular orbits:

$${}_{-2}C_{2\pm 2}(t) = 32\sqrt{\frac{\pi}{5}}\,\eta\,[M\omega(t)]^{8/3}\,e^{\mp 2i(\varphi(t)-\varphi_0)} \qquad \varphi(t) = \int^t dt'\,\omega(t')$$

Equal-mass binary: *one* dominant frequency

- $\omega_c \Rightarrow$ **from the coordinate separation**
- $\omega_{\mathrm{D2}} = -\frac{1}{2}\mathrm{Im}\left[\frac{\dot{C}_{22}}{C_{22}}\right] \Leftarrow$ **from the wave**

Decoupling between orbital frequency and GW frequency

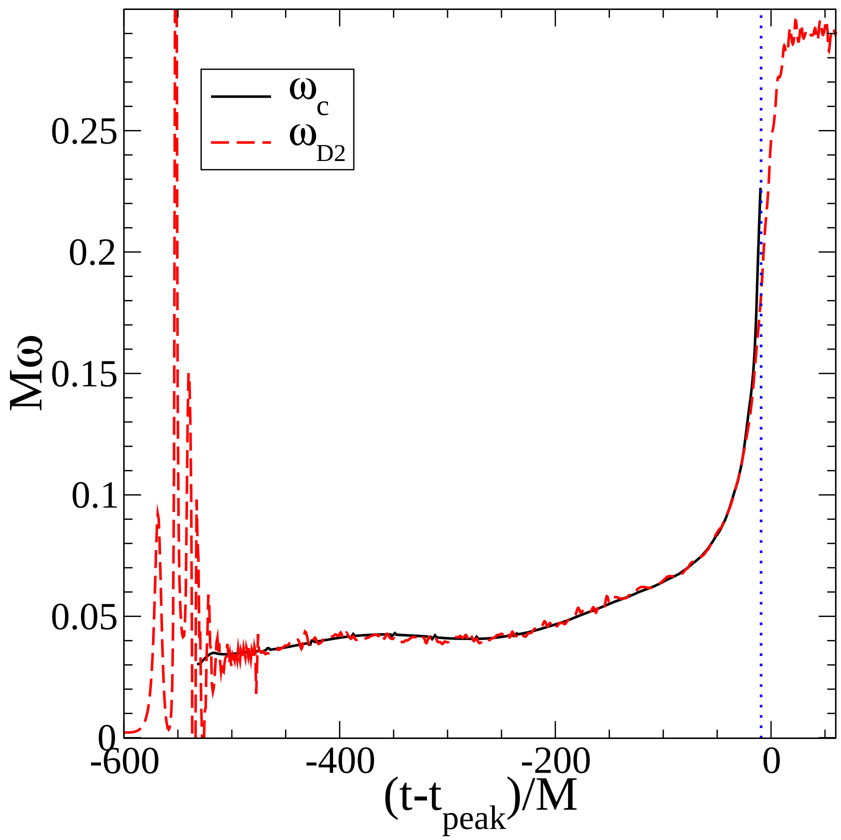

[AB, Cook & Pretorius 06]

When the ringdown phase starts. Higher overtones.

[AB, Cook & Pretorius 06; see also Berti et al. 07]

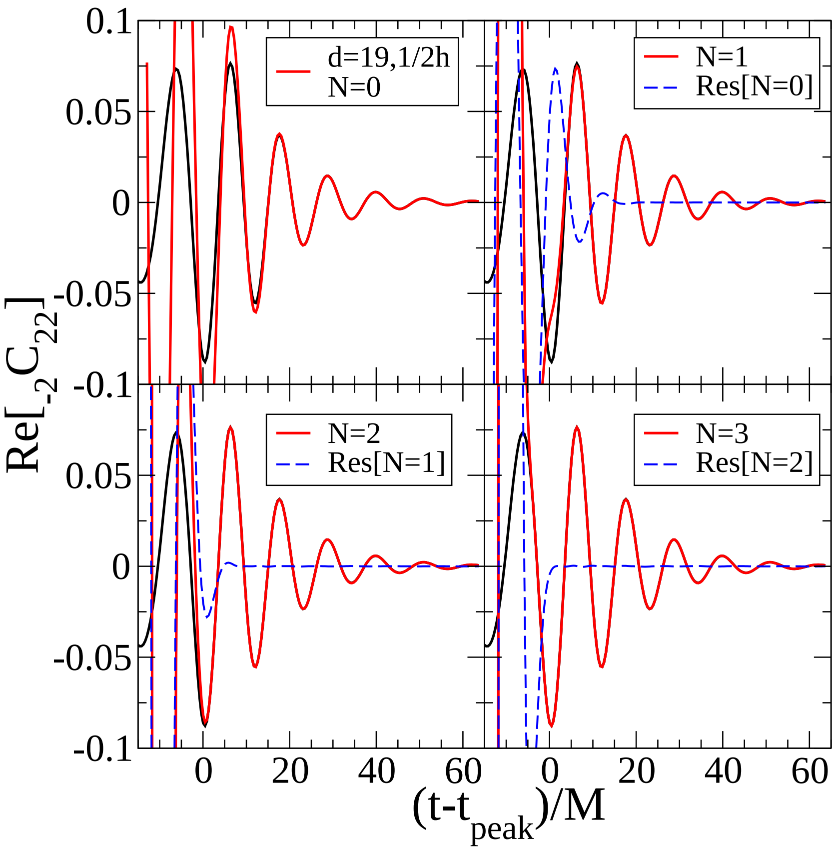

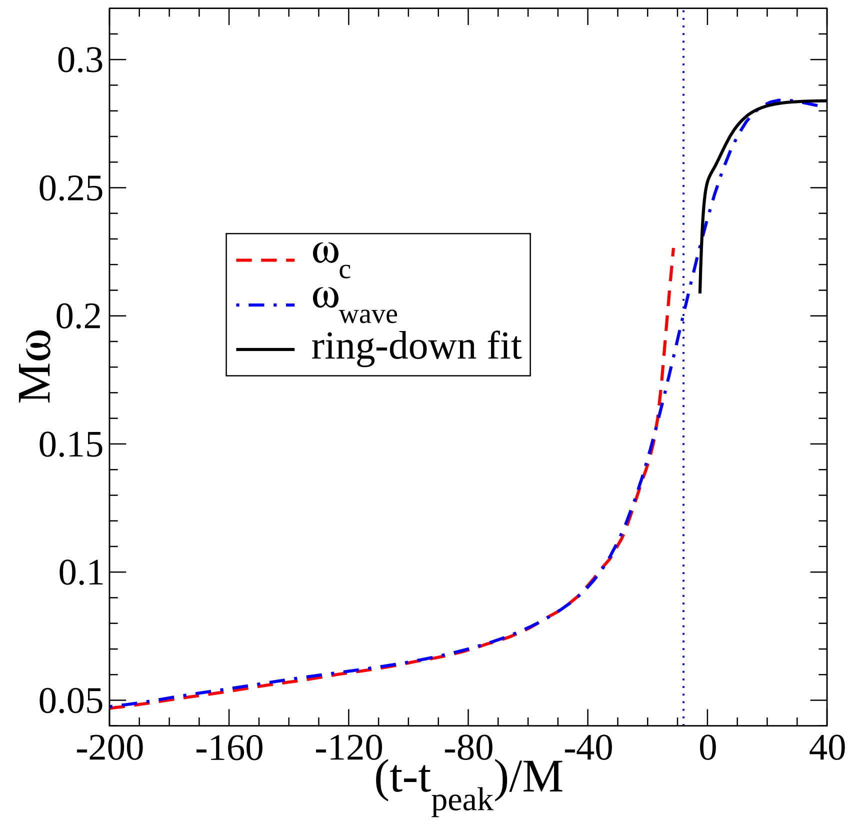

The (plunge and) merger

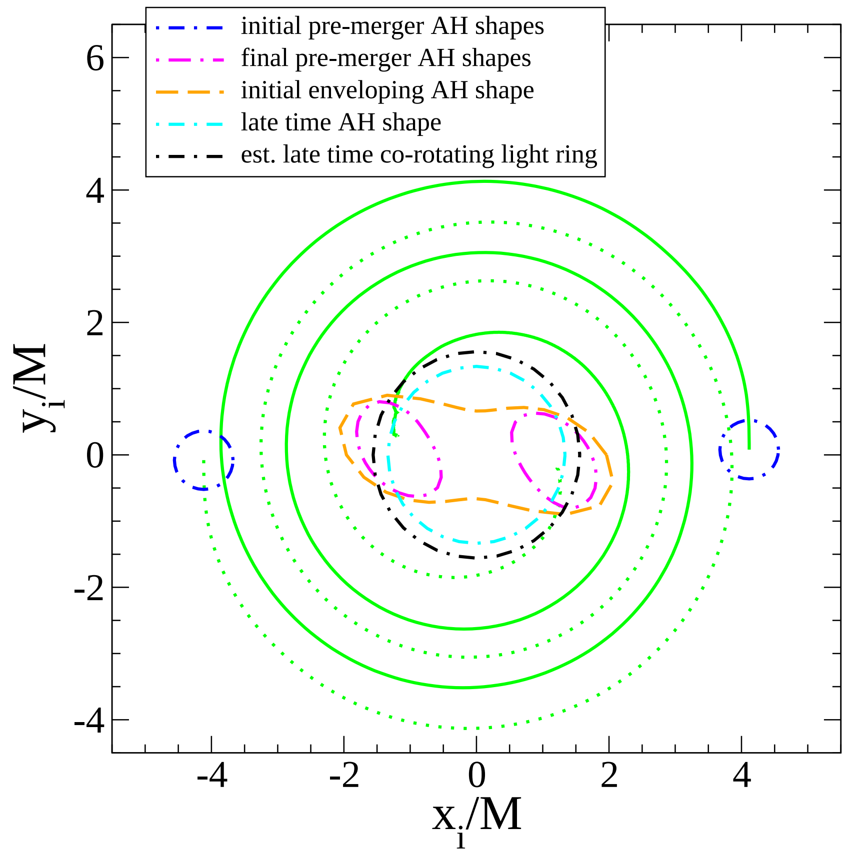

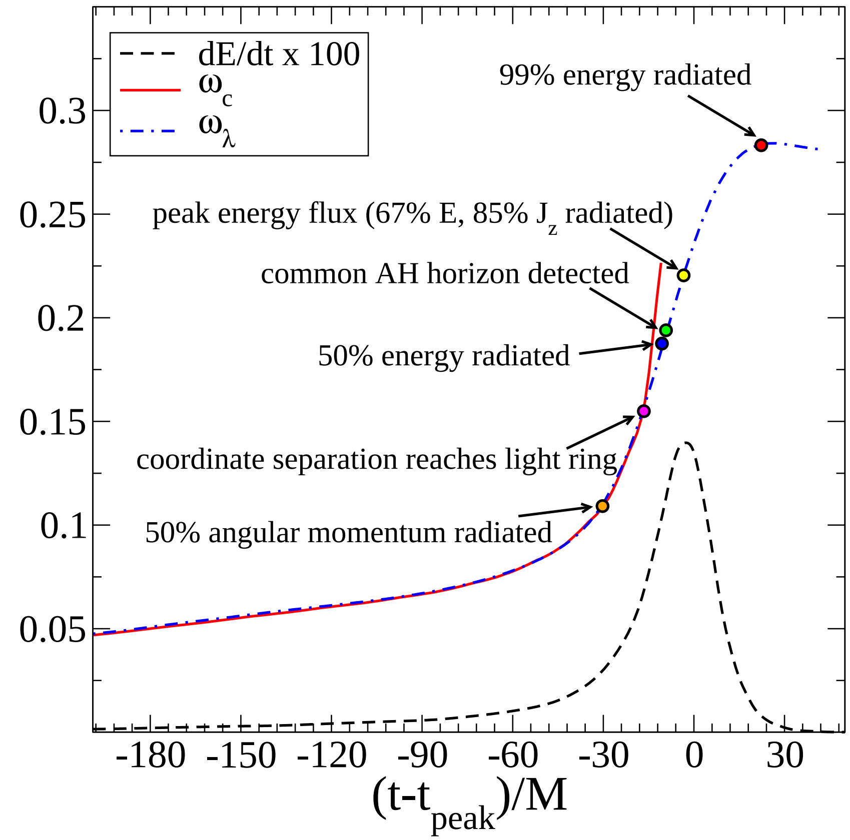

- *Short* **transition merger–ringdown**

[AB, Cook & Pretorius 06]

- **Energy and angular-momentum quickly released during merger**

Two separate issues

- **Less accurate templates (mild systematics) to** *detect the binary*

  $\Rightarrow$ *effective* **templates**

- **Very accurate templates (low systematics) to** *extract binary parameters*

  different accuracy is required if testing astrophysics or general relativity

  $\Rightarrow$ *faithful* **templates**

Significance of inspiral, merger and ringdown phases

[Pan, AB, Pretorius & NASA-Goddard 07]

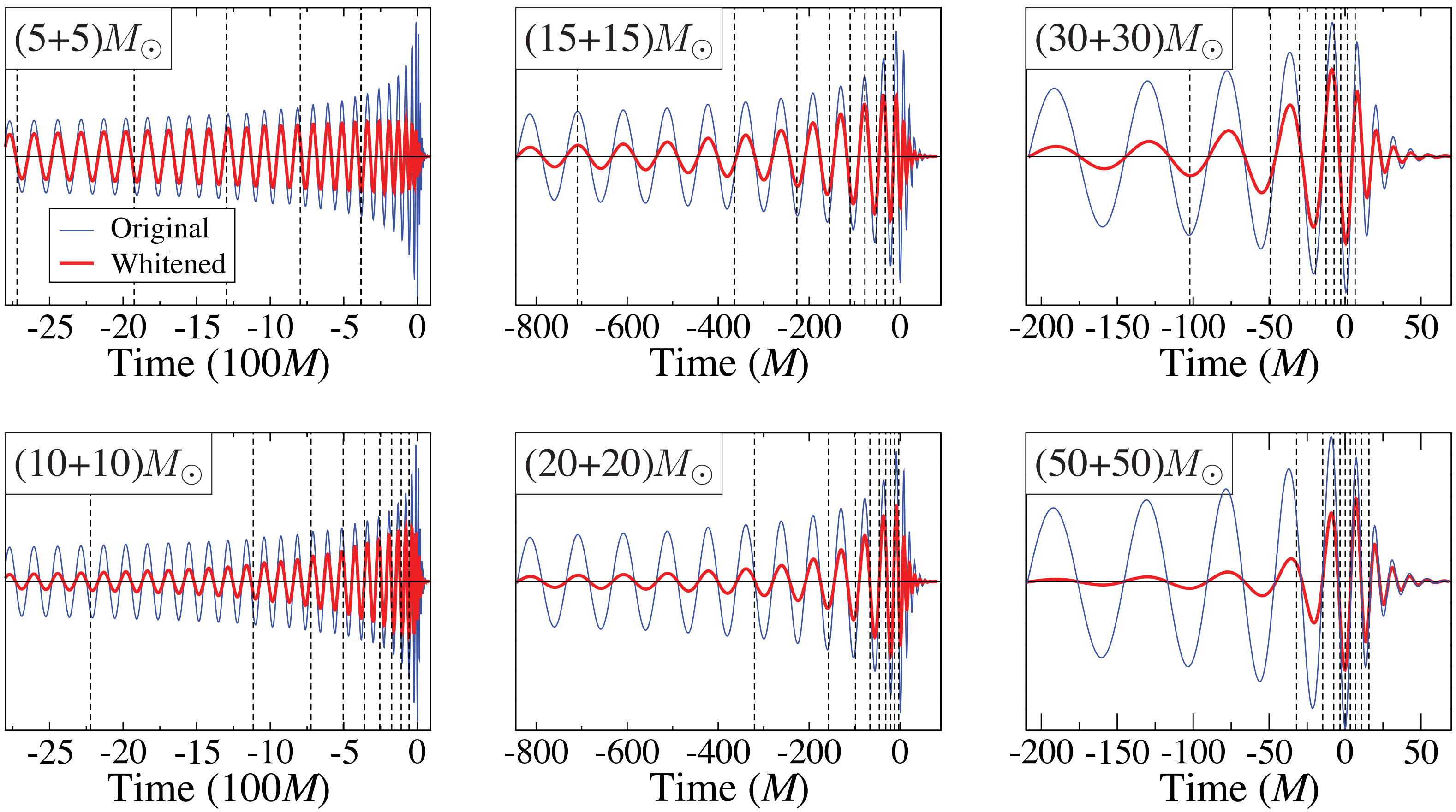

Comparison NR and PN/EOB approximants: data-analysis purposes

- Equal-mass case [Pan, AB, Pretorius & NASA-Goddard 07]

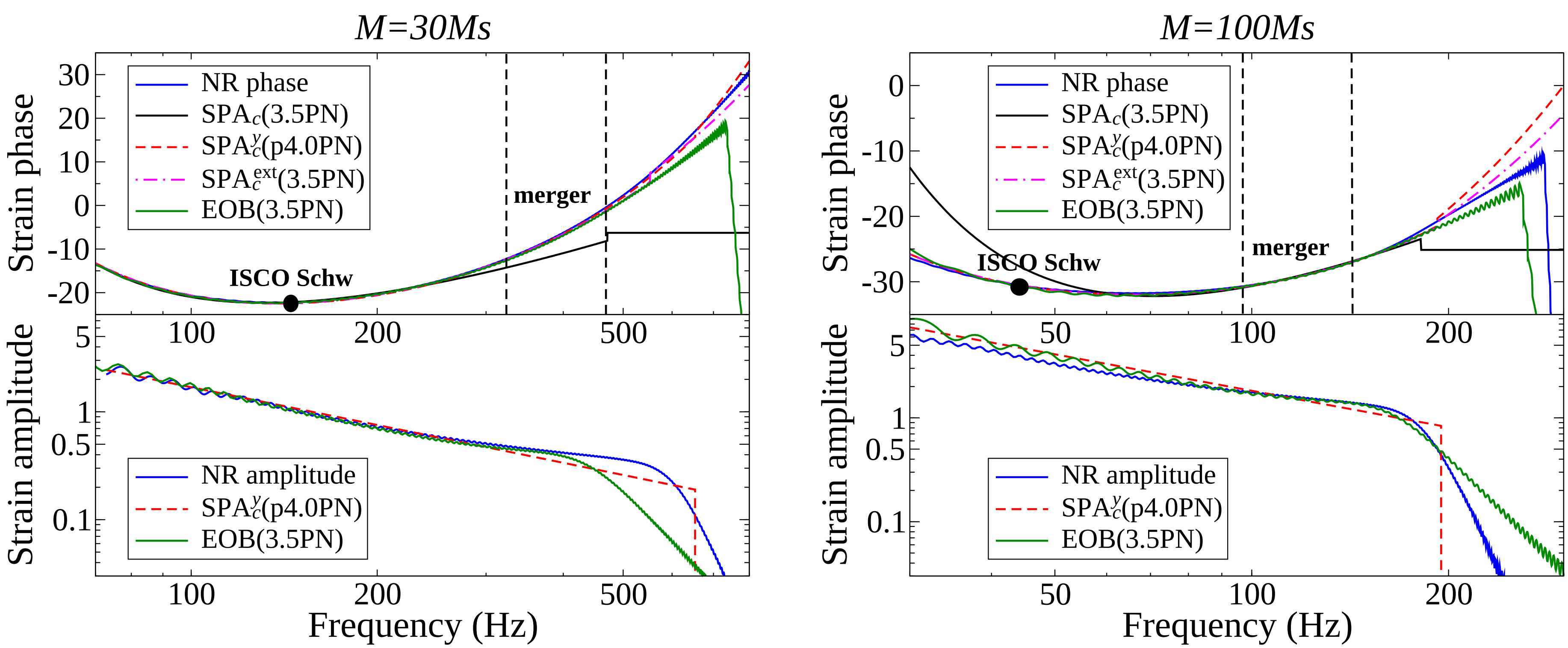

$\psi^{\rm SPA}_{\rm GW}(f) = 2\pi f t_0 - \phi_0 - \frac{\pi}{4} + \frac{3}{128\eta v^5}\sum_{k=0}^{N} \alpha_k v^k$ **with** $\alpha_8 = \mathcal{Y}\log v$ **and** $f_{\rm cut} = f^{\rm QNM}_{220}$

PN-approximants as *effective* templates

[Pan, AB, Pretorius & NASA-Goddard 07]

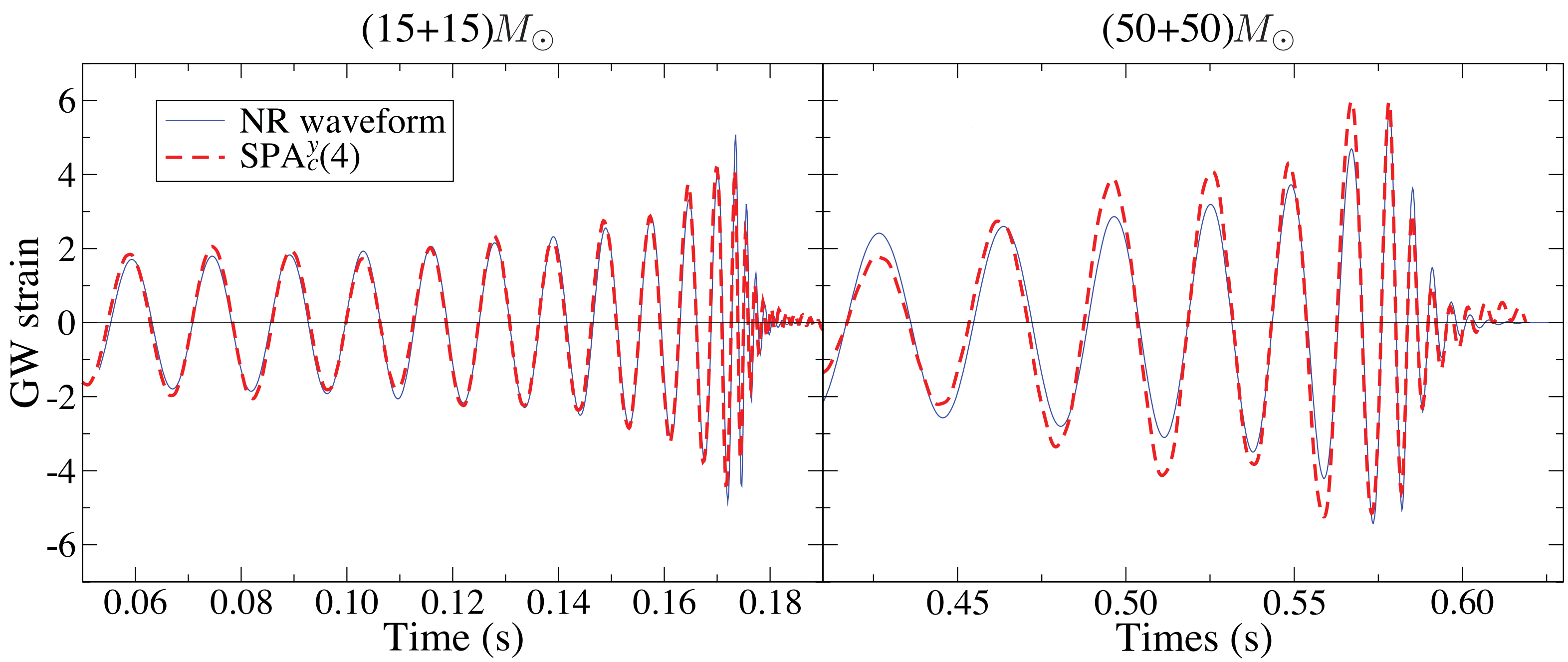

- **FF $\gtrsim$ 0.97 maximizing on binary parameters, time-of-arrival, initial phase**

Comparison NR and EOB model: full waveform

- $E_{\rm LR} = 0.97\, M$ **and** $J_{\rm LR}/E^2_{\rm LR} = 0.77$ [AB, Cook & Pretorius 06]
- **Fundamental QNM mode and two overtones included**

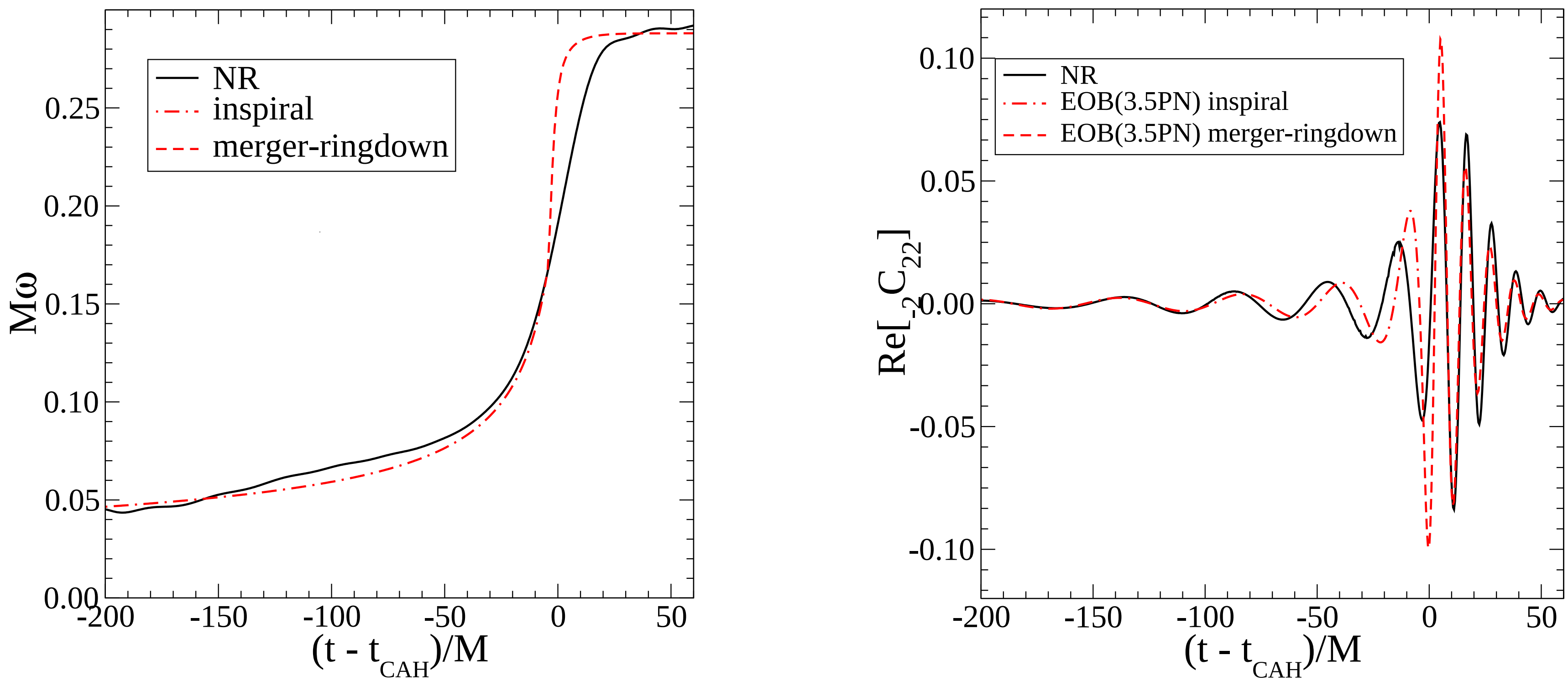

- **FF $\gtrsim$ 0.97 maximizing on binary parameters, time-of-arrival, initial phase**

Detectability for ground-based detectors

[AB, Cook & Pretorius 06; Baker et al. 06; Brady et al. 06; Pan, AB & NASA-Goddard 07]

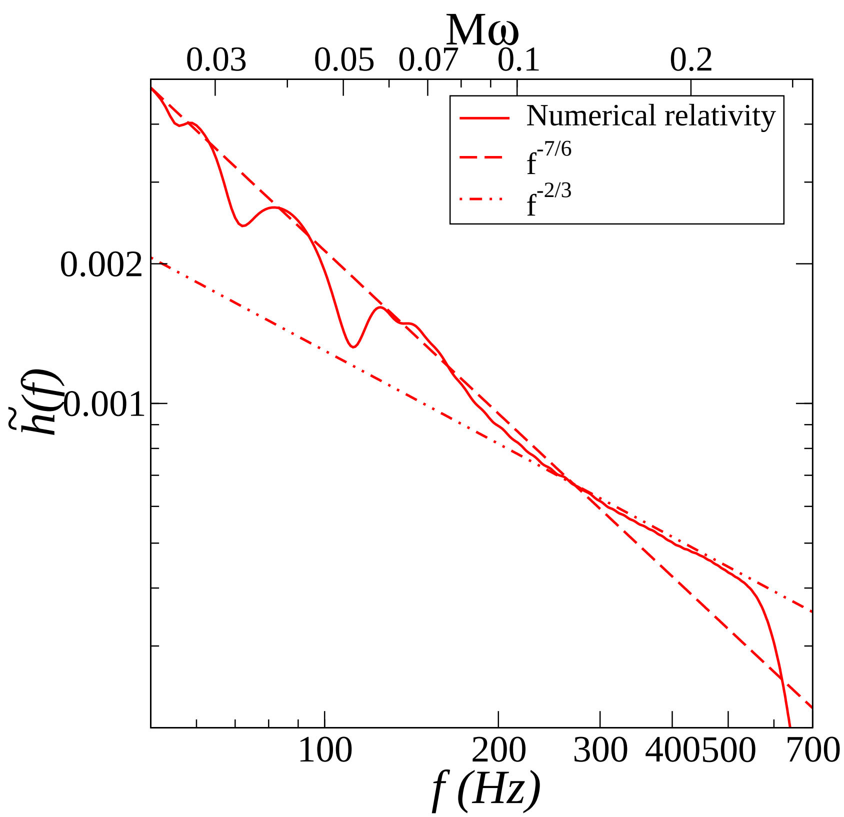

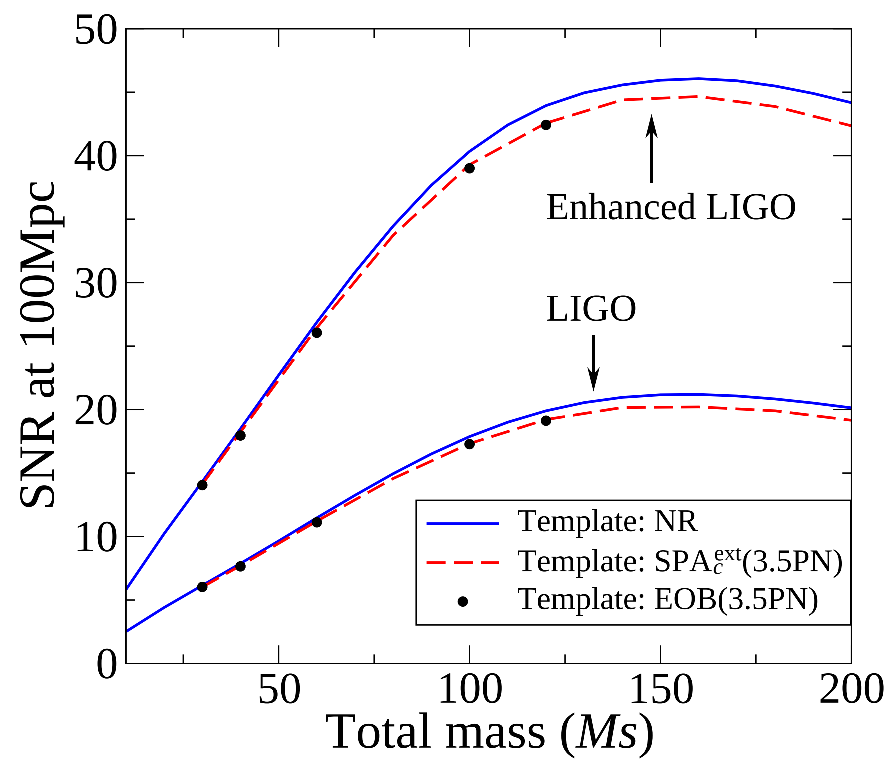

Change of slope: $f^{-7/6} \Rightarrow f^{\approx -2/3}$

increase of SNR for $M > 40 M_\odot$

Improved EOB model: modifying the EOB radial potential and determining final BH mass and spin from NR

[AB, Pan & NASA-Goddard 07]

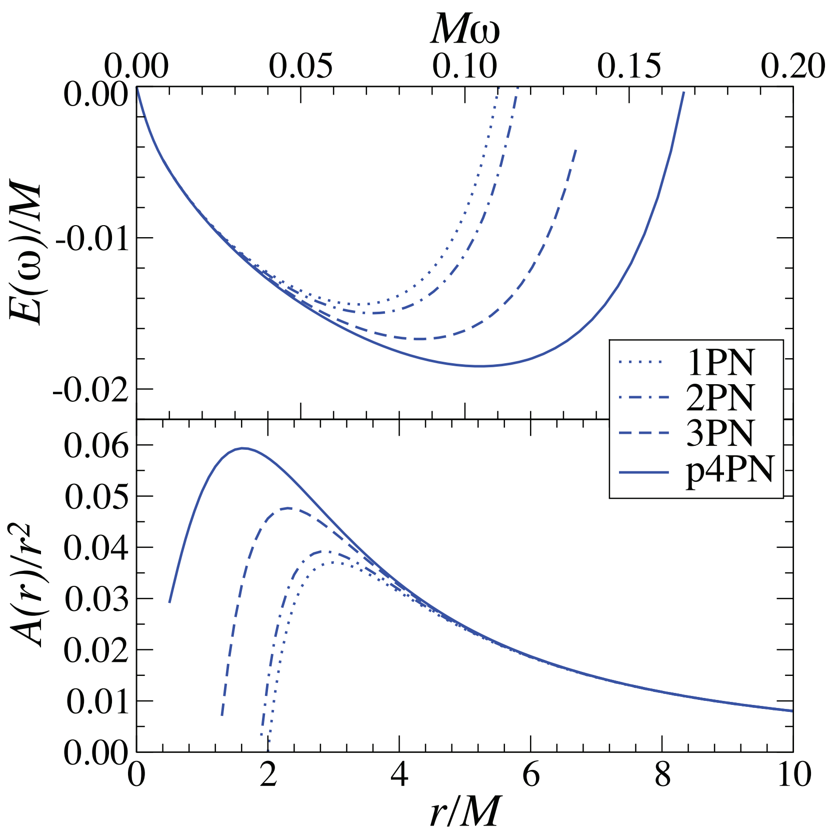

[Damour, Iyer, Jaranowski & Sathyaprakash 03]

- $A^{\rm p4PN}(r) = A^{\rm 3PN}(r) + \frac{\lambda\,\eta}{r^5}, \;\; \lambda = 60$
- **Apply Padé resummation to ensure presence of LSO and light ring**
- **Analytical matching point**

  $M\,\omega_{\rm match} = 0.133 + 0.183\,\eta + 0.161\eta^2$
- **QNM frequency and decay time depend** *only* **on** $M_{\rm BH}/M$ **and** $a_f/M_{\rm BH}$

  $M_{\rm BH}/M = 1 + (\sqrt{8/9} - 1)\,\eta - 0.498\,\eta^2$

  $a_f/M_{\rm BH} = \sqrt{12}\,\eta - 2.90\,\eta^2$

What determines the (non-adiabatic) frequency during the plunge?

[AB, Pan & NASA-Goddard 07]

- $\omega(t) = \frac{A(r)}{r^2} \frac{p_\varphi}{\eta \hat{H}_{\rm real} \hat{H}_{\rm eff}}$

- $\omega_{\rm plunge}(t) \simeq \frac{A(r)}{r^2}\, {\rm const}$

$${\rm const} = \left[\frac{p_\varphi}{\eta \hat{H}_{\rm real} \hat{H}_{\rm eff}}\right]_{\rm LSO}$$

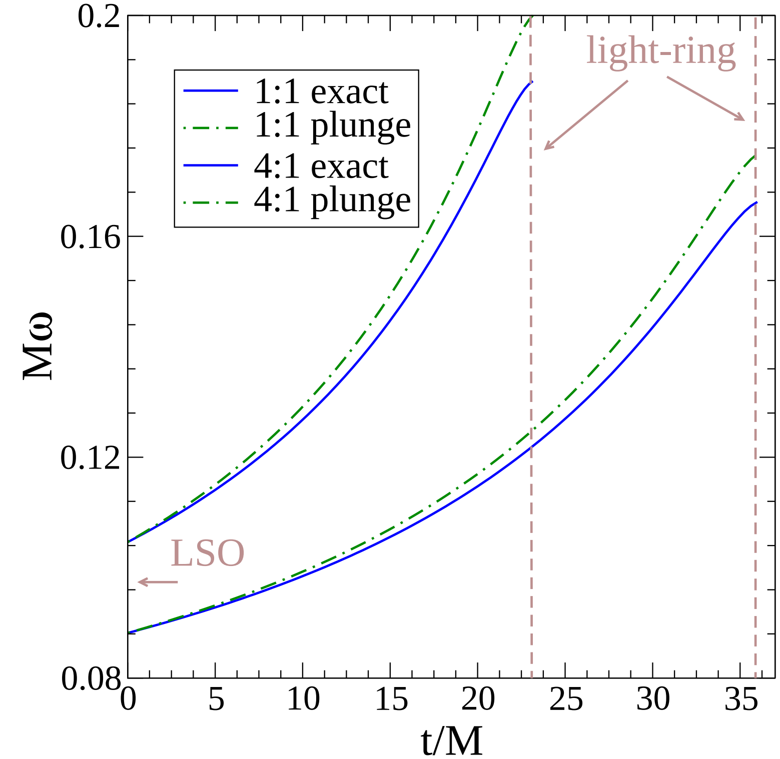

$\frac{A(r)}{r^2} \Rightarrow$ radial potential for a massless particle in Schwarzschild (light-ring)

Comparison NR and EOB(p4.0PN): equal-mass case

- **Phase difference in GW cycles of** $\sim 5\%$ [AB, Pan & NASA-Goddard 07]
- **FF** $\gtrsim 0.98$ **maximizing** *only* **on time-of-arrival and initial phase**

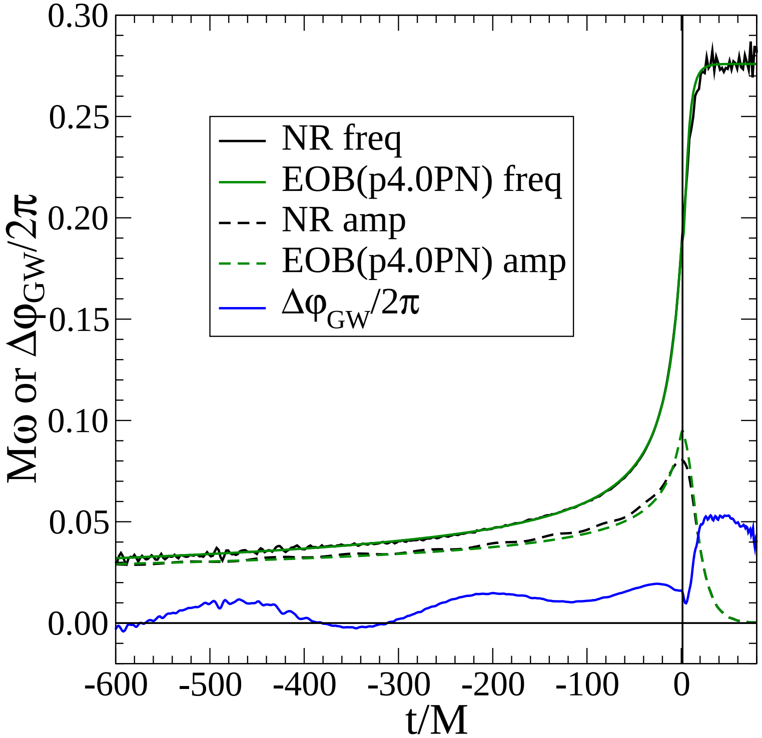

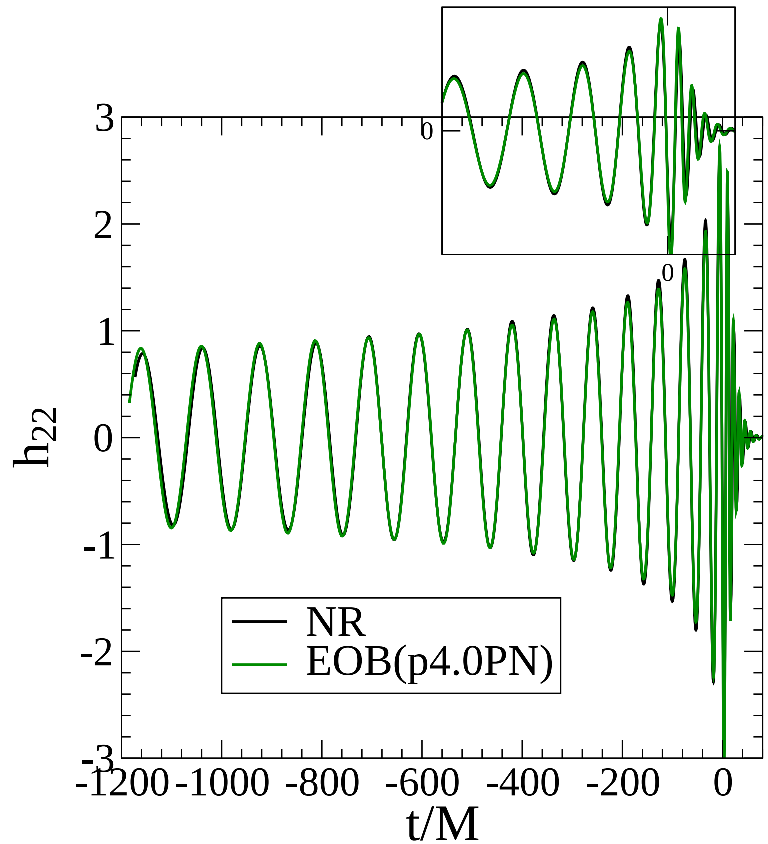

Unequal-mass binaries: several multipole moments

- **Mass ratio 4:1: modes with $l \neq 2$, $m \neq 2$ no longer sub-dominant**

[AB, Pan & NASA-Goddard 07]

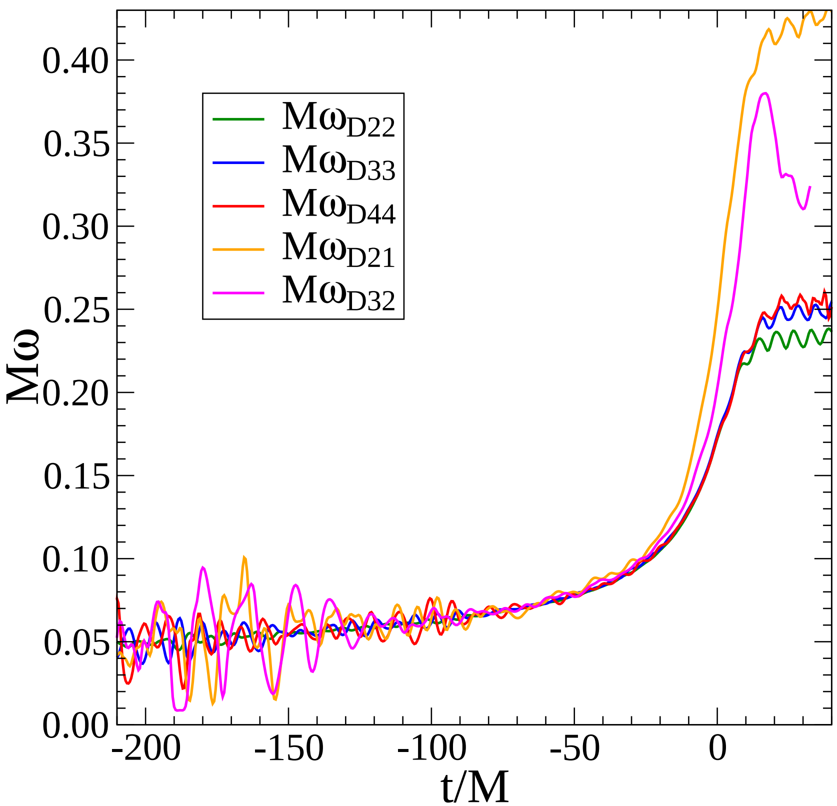

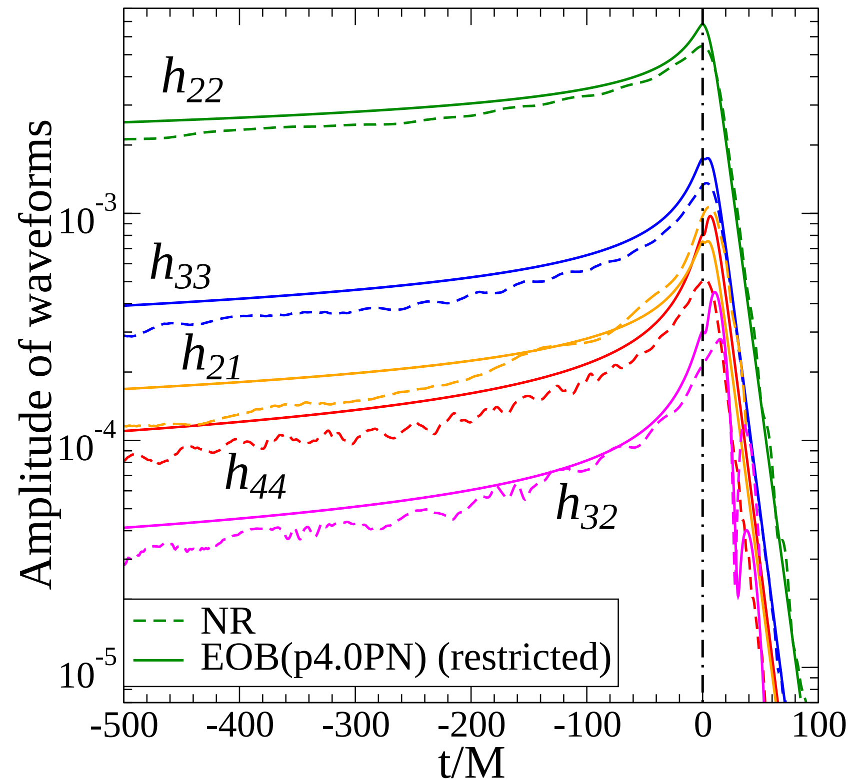

Comparison NR and p4PN-EOB model: unequal-mass case

- **Phase difference in GW cycles of** $\sim 8\%$ `[AB, Pan & NASA-Goddard 07]`
- **FF** $\gtrsim 0.98$ **maximizing** *only* **on time-of-arrival and initial phase**

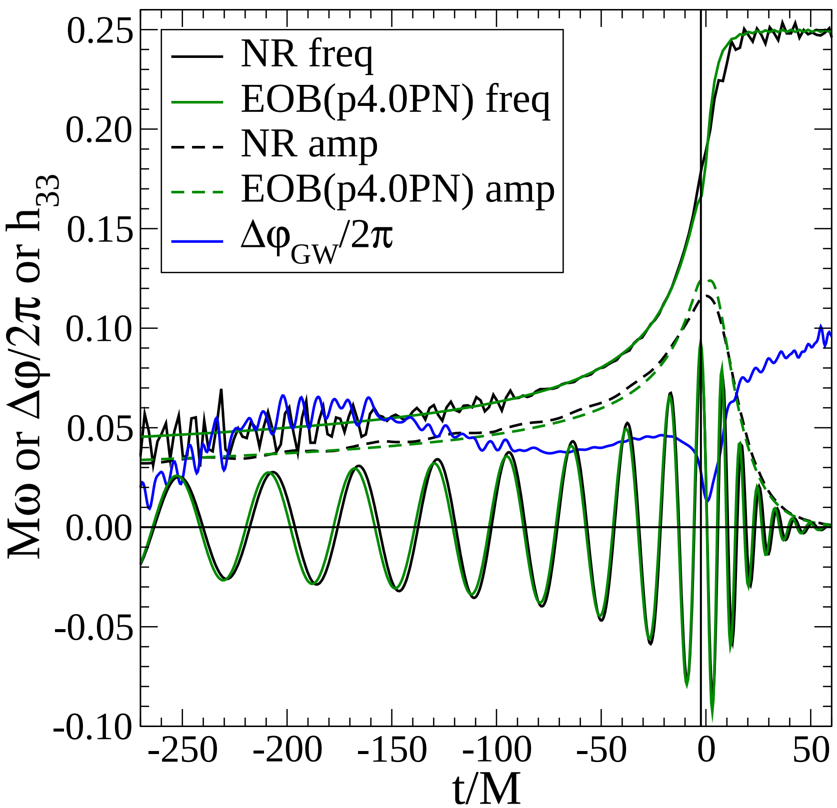

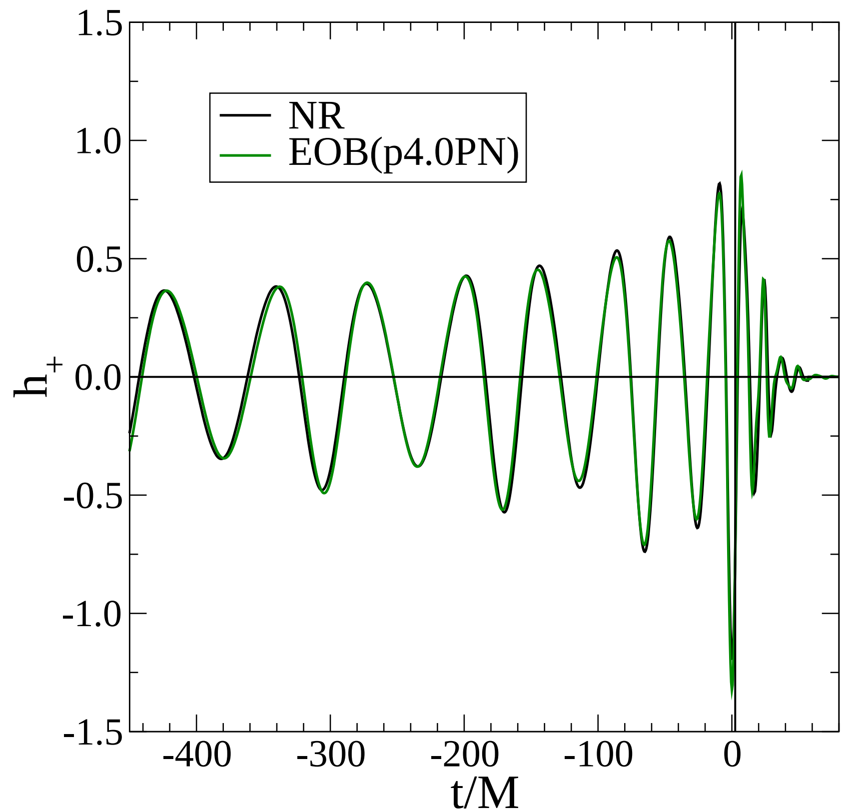

Suboptimal merger-ringdown match for subdominant modes

[AB, Pan & NASA-Goddard 07]

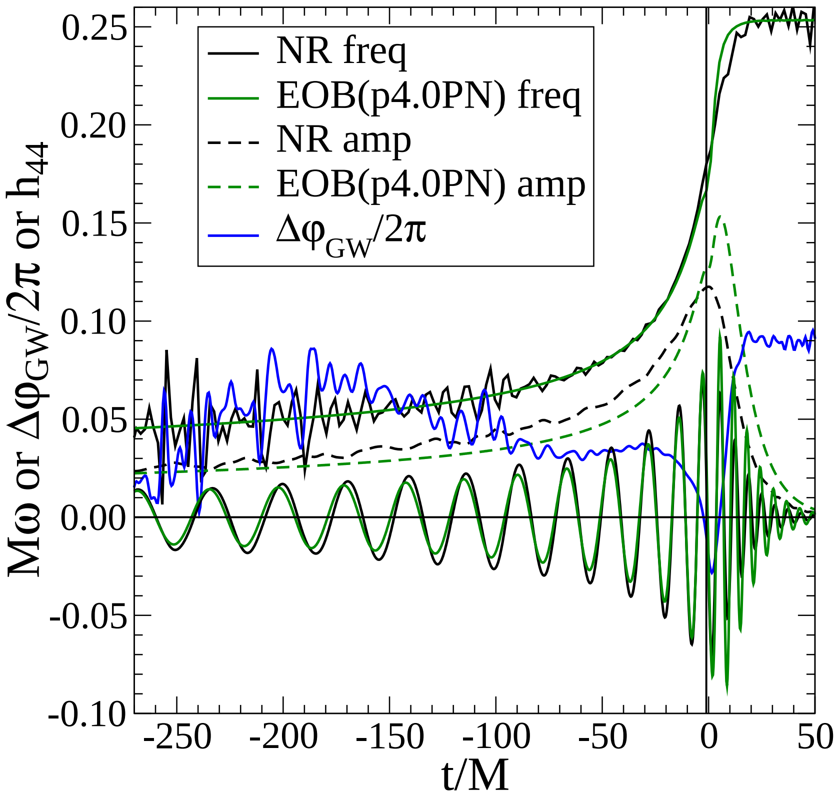

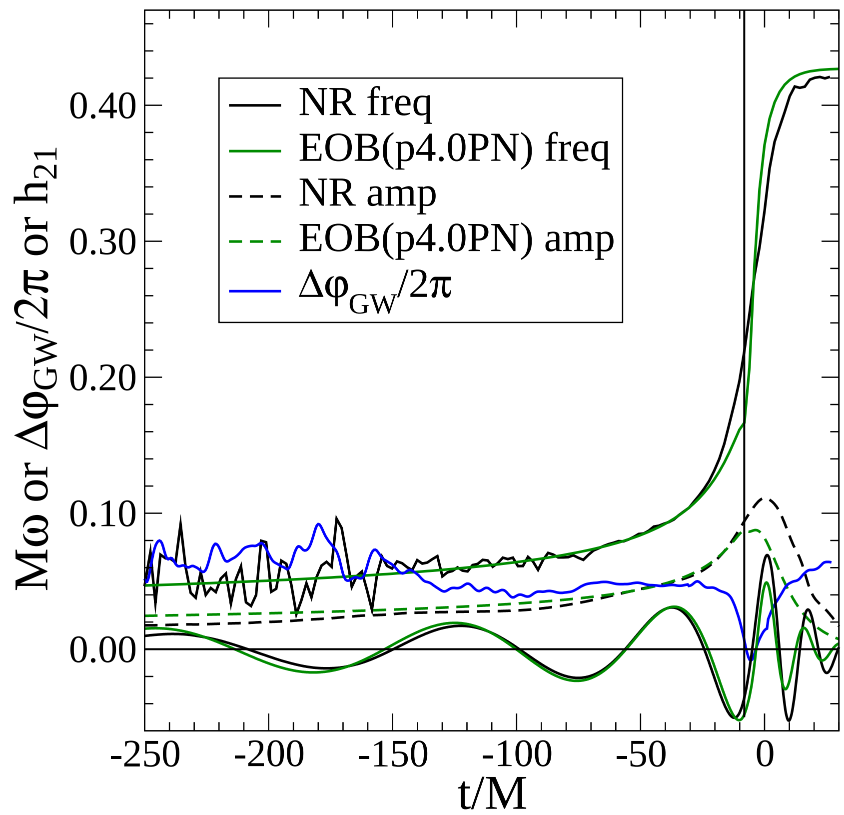

Comparison Regge-Wheeler and EOB model in the test-mass limit

[Damour, Nagar & Tartaglia 06; Damour & Nagar 07]

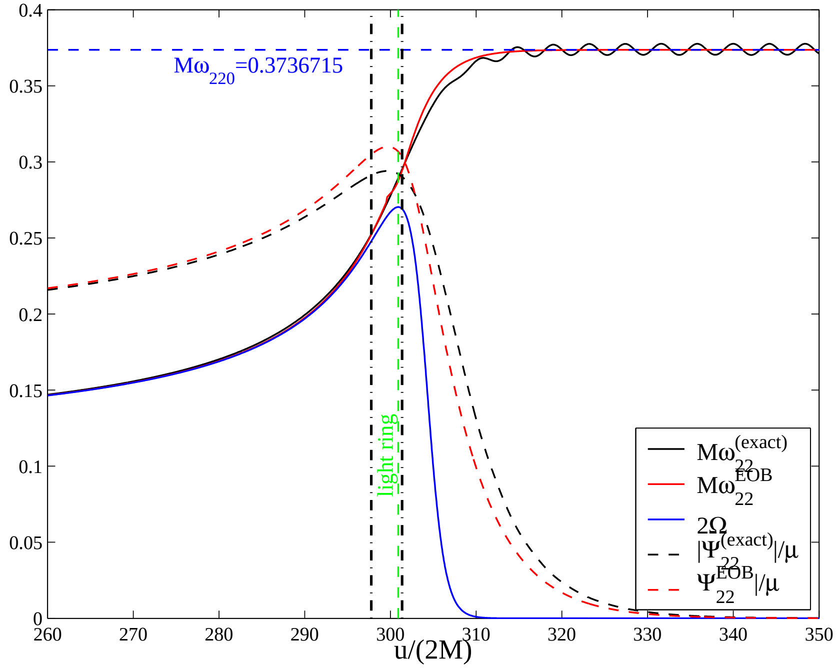

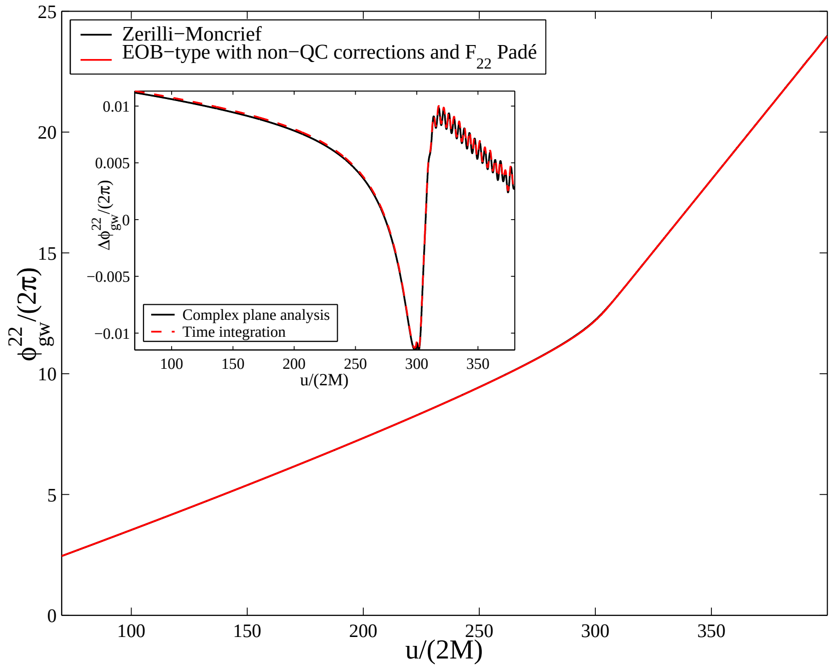

- **Several improvements: resummed higher-order amplitude corrections; deviations from quasi-circular motion; matching on a *comb* instead of a point**

Comparison EOB(3.5PN) and extremely accurate NR waveforms

[Pan & AB]

- $\omega_{\rm in} = 0.016$
- **freq and phase matched at** $\omega_{\rm match} = 0.02$
- $\omega_{\rm fin} = 0.05$
- **Total number of of GW cycles** ~ 30

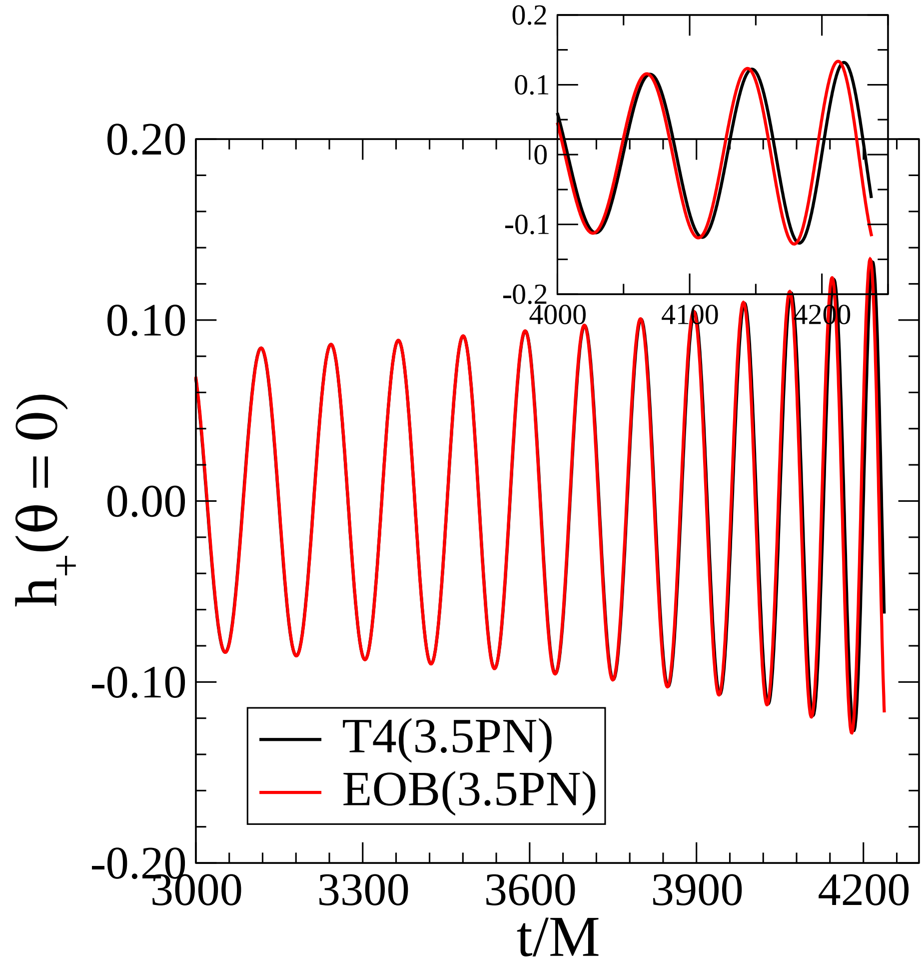

Comparison EOB and extremely accurate NR waveforms

$\omega_{\rm in} = 0.016$, **freq and phase matched at** $\omega_{\rm match} = 0.02$ **and** $\omega_{\rm fin} = 0.05$

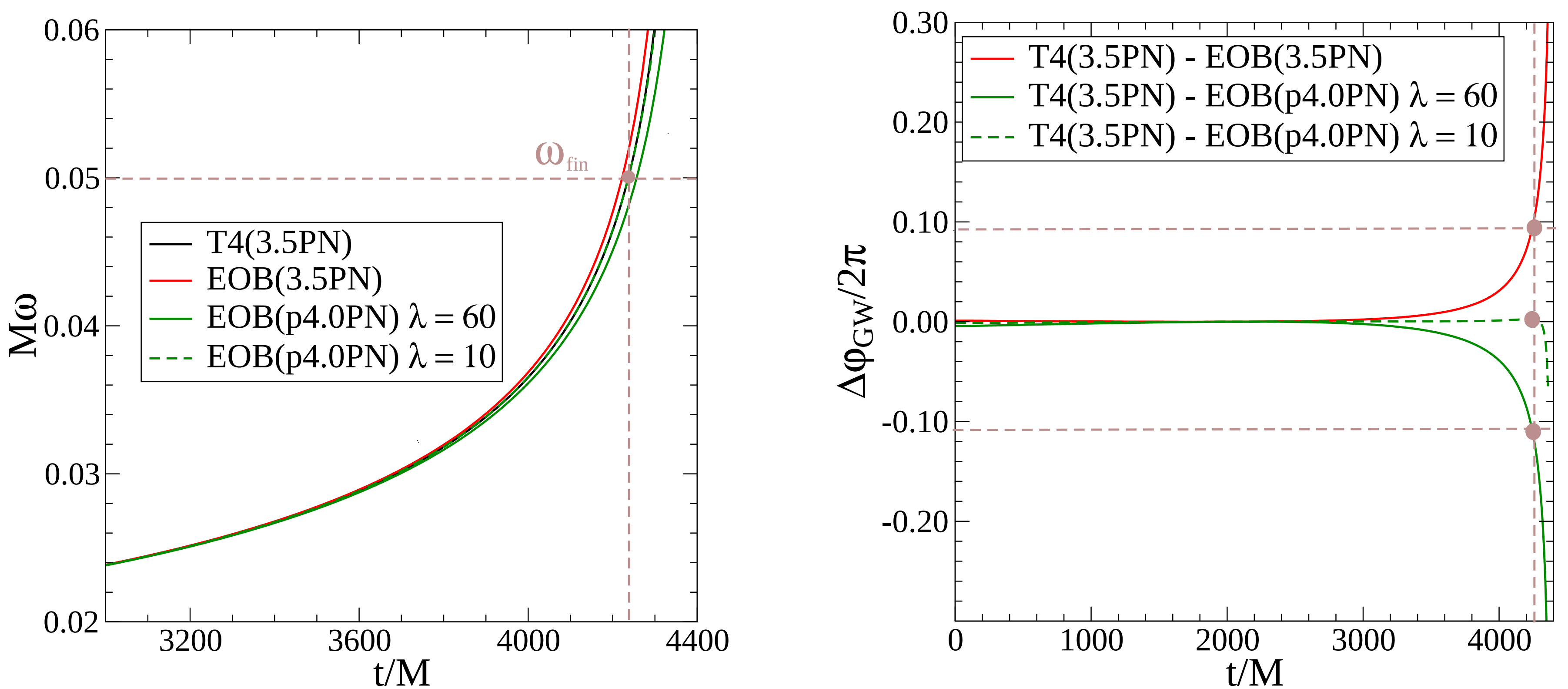

$(\Delta\varphi)_{\rm EOB(3.5PN)} = 0.27\,{\rm rad}$

[Pan & AB] $(\Delta\varphi)^{\lambda=60}_{\rm EOB(p4.0PN)} = -0.32\,{\rm rad}$, $(\Delta\varphi)^{\lambda=10}_{\rm EOB(p4.0PN)} = 0.01\,{\rm rad}$

Example of EOB(p4.0PN) matching the extremely accurate NR waveforms and going beyond it!

$\omega_{\rm in} = 0.016$, **freq and phase matched at** $\omega_{\rm match} = 0.02$ [Pan & AB]

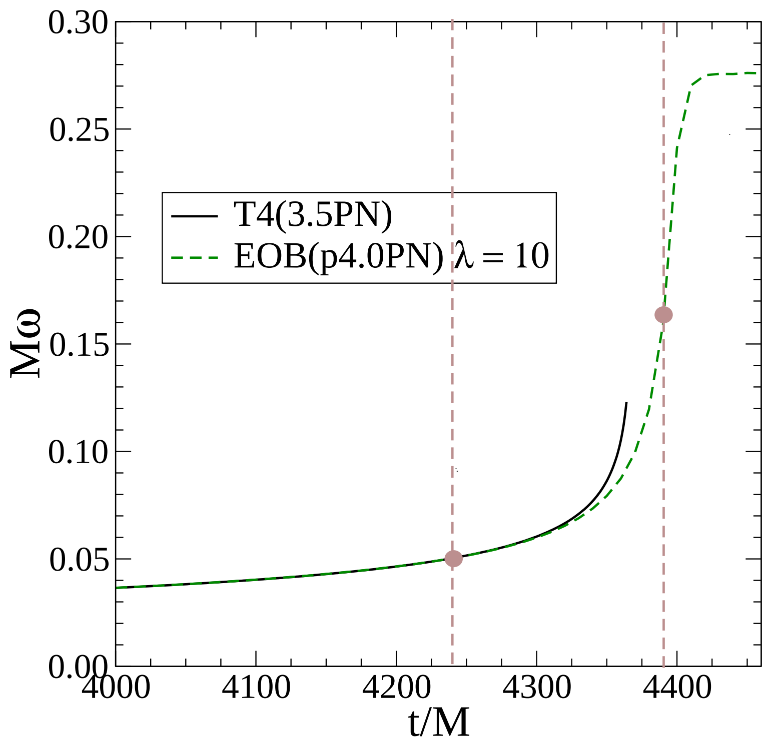

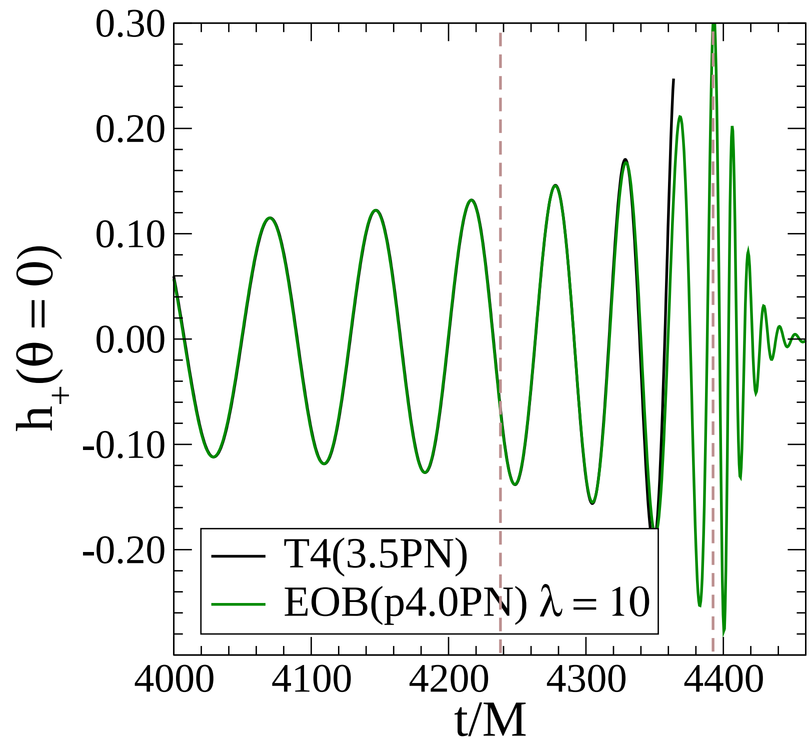

Comparison EOB- and Taylor-approximants in presence of spin

[Pan & AB]

- $\omega_{\rm in} = 0.02$
- **freq and phase matched at** $\omega_{\rm in} = 0.02$
- $\omega_{\rm fin} = 0.05$
- **Total number of of GW cycles** ~ 20

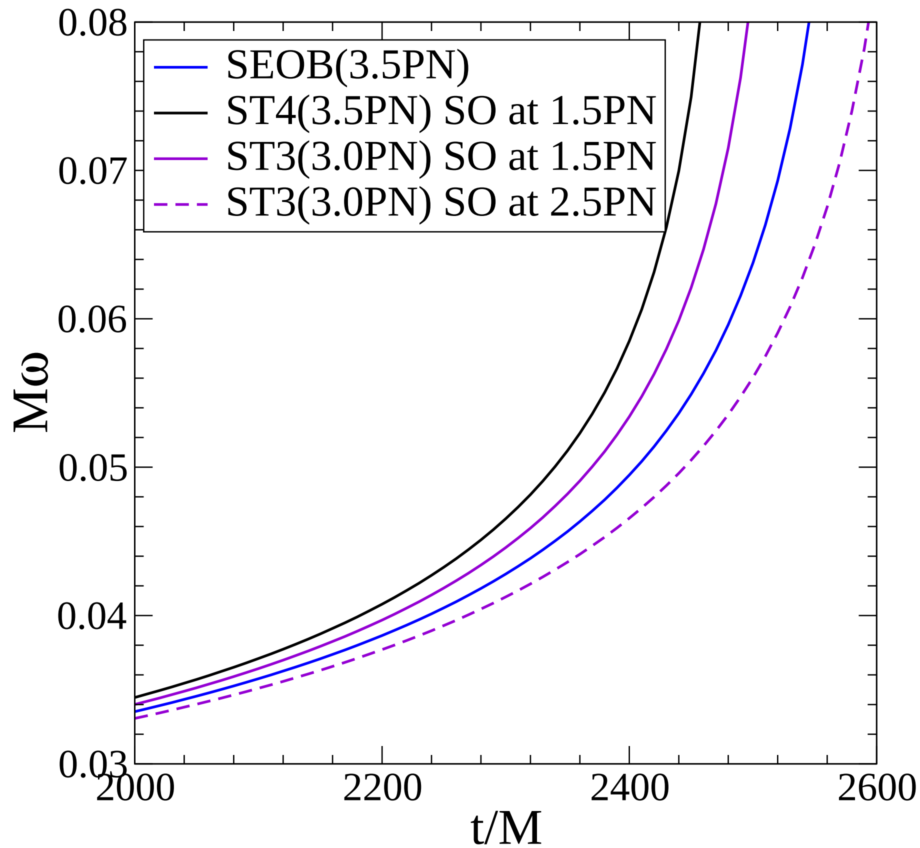

- **We need higher-order PN spin corrections!**

Predictions for gravitational recoil using analytical calculations

GWs bring away binary's energy, angular momentum and *linear momentum*:

$$\frac{d\mathbf{P}}{dt} \sim \frac{1}{c^7}\left(I^{22}\,S^{21} + I^{22}\,I^{33} + \frac{1}{c^2}\,I^{33}\,I^{44} + \cdots\right)$$

$I^{22} \Rightarrow$ mass quadr., $I^{33} \Rightarrow$ mass octup.

$S^{21} \Rightarrow$ current quadr., $I^{44} \Rightarrow$ mass hexad.

- **PN predictions consistent with NR throughout inspiral** [Blanchet et al. 06]
- **Final kick determined by the short-merger/ringdown transition ⇒ importance of including the ringdown phase** [Damour & Gopakumar 06]
- **PN kick formula for quasi-circular orbits** [Kidder 95]

$$|\mathbf{V}| = \mathcal{A}\,\frac{q^2}{(1+q)^5}\,\sqrt{\mathcal{B}\,(1-q)^2 + 2\mathcal{C}\,(1-q)\,K_{\rm planar} + \mathcal{D}\,K^2_{\rm planar} + \mathcal{E}\,K^2_{\rm nonplanar}}$$

$K_{\rm planar} = q\,\chi_2\,\cos\theta_2 - \chi_1\,\cos\theta_1 \quad K_{\rm nonplanar} = q\,\chi_2\,\sin\theta_2\,\cos\phi_2 - \chi_1\,\sin\theta_1\,\cos\phi_1$

$\theta_{1,2} \Rightarrow$ angle between the spin and orbital angular-momentum $\qquad q = m_1/m_2$

$\phi_{1,2} \Rightarrow$ azimuthal angle of each spin, measured with respect to the binary separation vector

Large kicks for equal-mass binaries

Total spin equal to zero; spins on the orbital plane

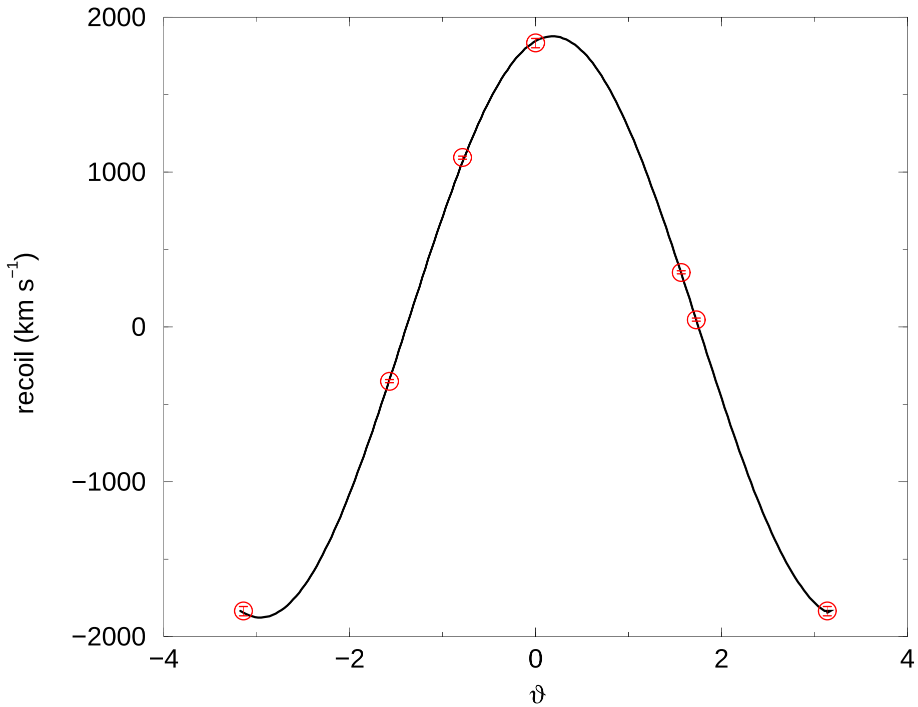

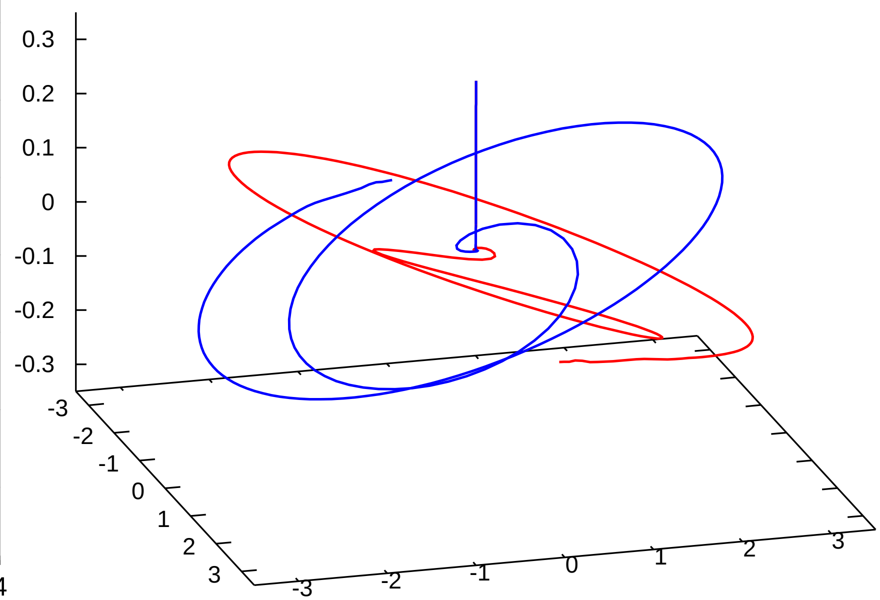

several recent results from `UTB/RIT, Jena U, Florida Atlantic U, Penn State/Austin U`

Anatomy of the kick (inspiral–merger–ringdown)

[Schnittman, AB & NASA-Goddard 07]

$$|\mathbf{V}_{\rm kick}| \simeq \int \left[\hat{\mathbf{V}} \cdot \frac{d\mathbf{P}}{dt}(I^{22}\, S^{21}) + \hat{\mathbf{V}} \cdot \frac{d\mathbf{P}}{dt}(I^{22}\, I^{33}) + \hat{\mathbf{V}} \cdot \frac{d\mathbf{P}}{dt}(I^{33}\, I^{44})\right] dt$$

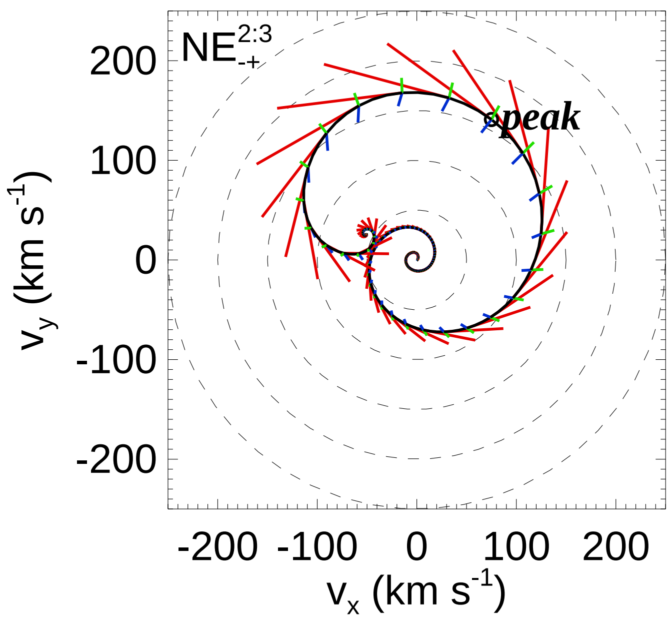

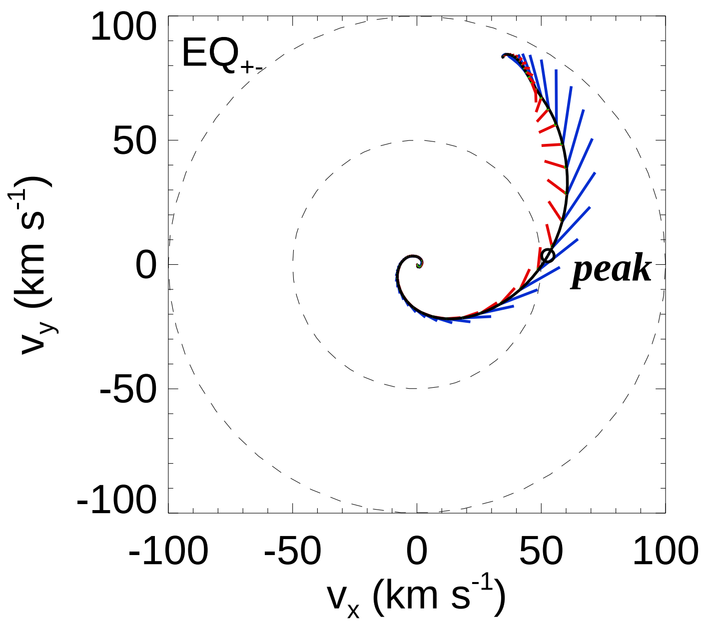

Anatomy of the kick and anti-kick

[Schnittman, AB & NASA-Goddard 07]

- **Magnitude of anti-kick depends on QNM-frequencies associated to dominant modes**

$I^{22}\, I^{33\,*}$: $(\omega_{33}^{\rm QNM} - \omega_{22}^{\rm QNM})$ **is large** $\Rightarrow$ **spiral back inward**

$I^{22\,*}\, S^{21}$: $(\omega_{21}^{\rm QNM} - \omega_{22}^{\rm QNM})$ **is small** $\Rightarrow$ **drifts off**

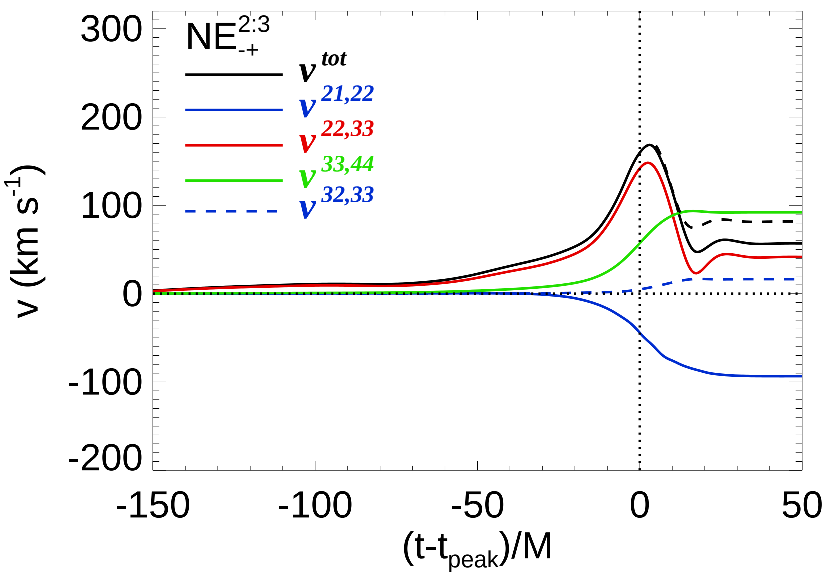

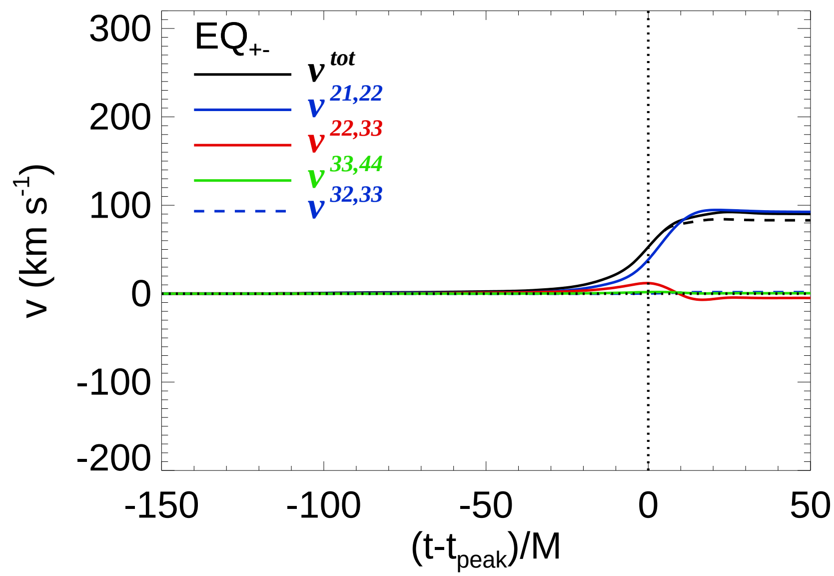

Cumulative probability distribution for recoil velocities using EOB approach

[Schnittman & AB 07]

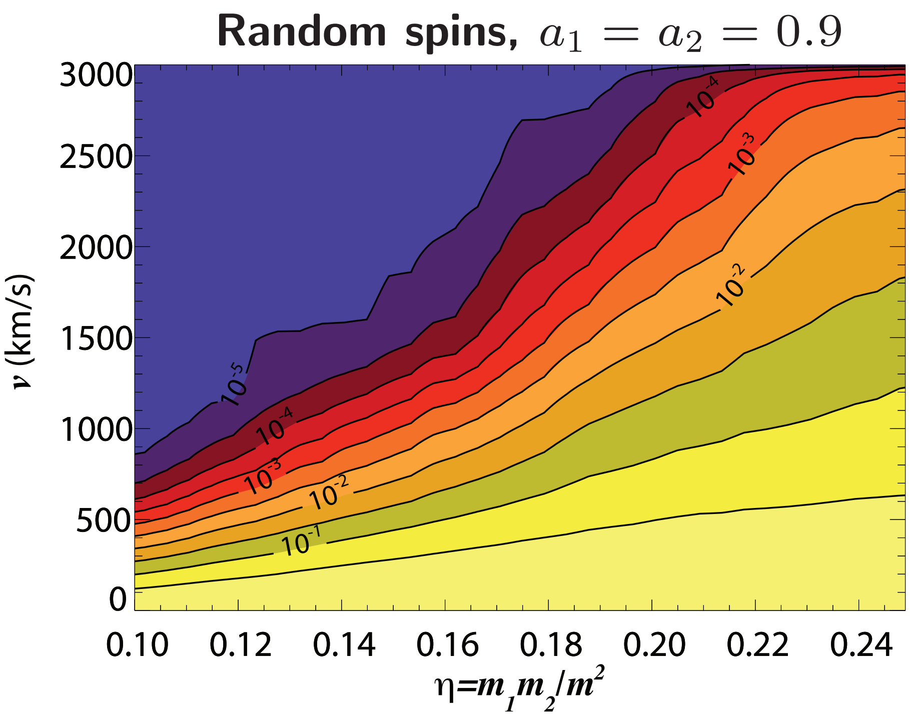

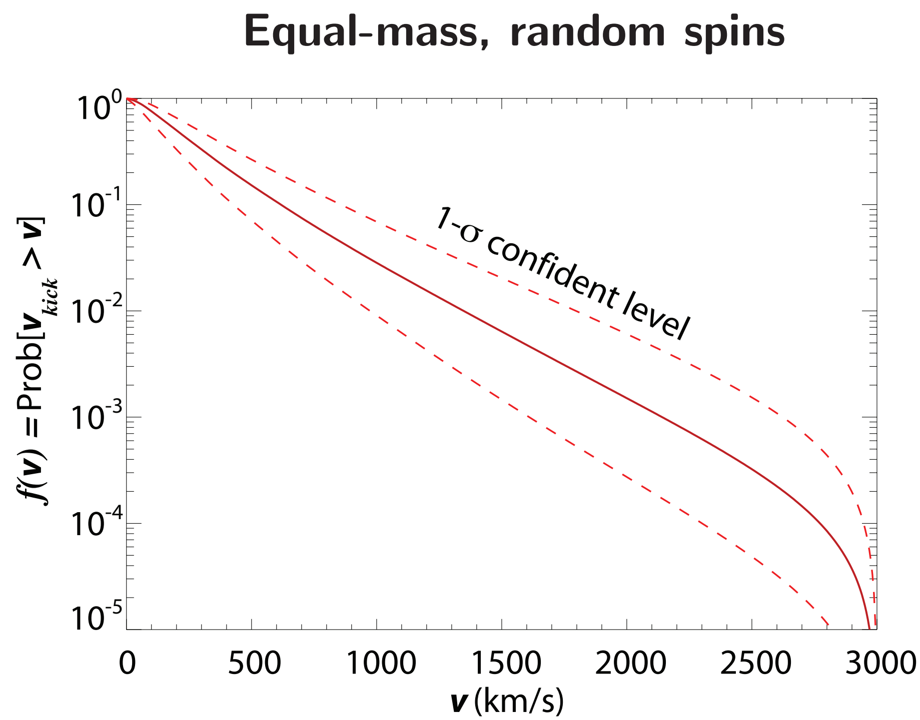

$$f_{v_{\rm kick}>500} = 0.12^{+0.06}_{-0.05}$$

$$f_{v_{\rm kick}>1000} = 0.027^{+0.021}_{-0.014}$$

Conclusions

- **Intriguing (anticipated) *simplicity* of (non-spinning) binary coalescence: details of merger hidden behind the curvature potential barrier.**

- **Relevant to dig out the curvature potential from numerical simulations.**

- **EOB/Padé resummations can condense the dynamics in a few functions $\Rightarrow$ natural flexibility to be employed for building an analytic model for the full waveform.**

- **Guided by NR simulations and by PN theory (at earlier times), notably the EOB model, we have a first example of analytical model for inspiral, merger, and ringdown *to be further improved* and extended to a larger class of binaries.**

- **Gravitational recoil determined mainly by merger-ringdown phases.**

- **Improvement of analytic modeling to reduce uncertainties in Monte Carlo simulations of recoil velocity distribution.**